



Protect Your Process

Eppendorf CO₂ incubators and Cell Culture Consumables

Features such as the seamless chamber make Eppendorf CO₂ incubators easy to clean and ensure a contamination-free environment. Eppendorf plates, dishes, and flasks facilitate your workflows while providing better security and consistency.

- > One piece seamless chamber in CO₂ incubator minimizes contamination risk and simplifies cleaning
- > Flasks with optimized protection against contamination by high efficiency air filter technology
- > SplashProtect™ ring inside of the dish lid traps liquid and prevents spills

www.eppendorf.com • 800-645-3050

Neural Stem Cell Grafts Promote Astroglia-Driven Neurorestoration in the Aged Parkinsonian Brain via Wnt/ β -Catenin Signaling

FRANCESCA L'EPISCOPO,^a CATALDO TIROLO,^a LUCA PERUZZOTTI-JAMETTI,^b MARIA F. SERAPIDE,^c NUNZIO TESTA,^a SALVATORE CANIGLIA,^a BEATRICE BALZAROTTI,^b STEFANO PLUCHINO,^b BIANCA MARCHETTI ^{a,c}

Key Words. Astrocyte–neuron crosstalk • Parkinson's disease • Wnt/ β -catenin signaling • Neural stem cells transplantation • Neuroinflammation • Brain plasticity

^aOasi Research Institute-IRCCS, Troina, Italy; ^bDept of Clinical Neurosciences, Clifford Allbutt Building - Cambridge Biosciences Campus and NIHR Biomedical Research Centre, University of Cambridge, Hills Road, CB2 0HA Cambridge, UK; ^cDepartment of Biomedical and Biotechnological Sciences (BIOMETEC), Pharmacology and Physiology Sections, University of Catania Medical School, Catania, Italy

Correspondence: Bianca Marchetti, Ph.D., Department of Biomedical and Biotechnological Sciences (BIOMETEC), Pharmacology Section, University of Catania Medical School, 64, 95125 Catania, Italy. Telephone: 3355722698; e-mail: biancamarchetti@libero.it; or Stefano Pluchino, M.D., Ph.D., Department of Clinical Neurosciences, Clifford Allbutt Building - Cambridge Biosciences Campus and NIHR Biomedical Research Centre, University of Cambridge, Cambridge CB2 0HA, United Kingdom. Telephone: +44-1223762042; e-mail: spp24@cam.ac.uk

Received August 25, 2017; accepted for publication March 6, 2018; first published online in *STEM CELLS EXPRESS* March 25, 2018.

<http://dx.doi.org/10.1002/stem.2827>

ABSTRACT

During aging—one the most potent risk factors for Parkinson's disease (PD)—both astrocytes and microglia undergo functional changes that ultimately hamper homeostasis, defense, and repair of substantia nigra pars compacta (SNpc) midbrain dopaminergic (mDA) neurons. We tested the possibility of rejuvenating the host microenvironment and boosting SNpc DA neuronal plasticity via the unilateral transplantation of syngeneic neural stem/progenitor cells (NSCs) in the SNpc of aged mice with 1-methyl-4-phenyl-1,2,3,6-tetrahydropyridine-induced experimental PD. Transplanted NSCs within the aged SNpc engrafted and migrated in large proportions to the tegmental aqueduct mDA niche, with 30% acquiring an astroglial phenotype. Both graft-derived exogenous (ex-Astro) and endogenous astrocytes (en-Astro) expressed Wnt1. Both ex-Astro and en-Astro were key triggers of Wnt/ β -catenin signaling in SNpc-mDA neurons and microglia, which was associated with mDA neurorescue and immunomodulation. At the aqueduct–ventral tegmental area level, NSC grafts recapitulated a genetic Wnt1-dependent mDA developmental program, inciting the acquisition of a mature Nurr1⁺TH⁺ neuronal phenotype. Wnt/ β -catenin signaling antagonism abolished mDA neurorestoration and immune modulatory effects of NSC grafts. Our work implicates an unprecedented therapeutic potential for somatic NSC grafts in the restoration of mDA neuronal function in the aged Parkinsonian brain. *STEM CELLS* 2018; 00:000–000

SIGNIFICANCE STATEMENT

Aging is the leading risk factor for the development of Parkinson's disease (PD) but little is known on the effects of neural stem/progenitor cells (NSC) transplants in the aged PD brain. Here, L'Episcopo and coworkers studied the effects of unilateral transplantation of syngeneic somatic NSCs within the substantia nigra pars compacta (SNpc) of aged PD mice and report a striking ability of grafted NSCs to restore nigrostriatal functionality. They uncover a chief role of graft-derived astrocytes and Wnt/ β -catenin signaling targeting both the SNpc neurons and the aqueduct (Aq)-dopaminergic (DA) niche, modulating the activity of endogenous astrocytes and the innate immune response, with therapeutical implications for DA restoration in aged PD brain.

INTRODUCTION

Parkinson's disease (PD) is the most prevalent central nervous system (CNS) movement disorder and the second most common neurodegenerative disease. Although recent evidence suggests that PD might originate outside of the brain and affect both central and peripheral neurons [1], a characteristic feature of this disease is the progressive loss of midbrain dopaminergic (mDA) neurons of the substantia nigra pars compacta (SNpc), which results in reduced striatal dopamine [2].

The causes and mechanisms leading to mDA neuron demise in sporadic PD remain poorly understood. Current evidence indicates that they depend on a complex interaction of genetic susceptibility, environmental factors and, most importantly, aging [3–10]. Aging is indeed the leading risk factor for the development of PD, as with advancing age the function of the nigrostriatal DA system progressively declines leading to neurochemical, morphological and behavioral changes [7–10]. Aging exacerbates inflammation and oxidative stress, which are crucial hallmarks of PD and 1-methyl-4-

phenyl-1,2,3,6-tetrahydropyridine (MPTP)-induced PD [4, 11–19], affecting plastic and regenerative responses [2, 7–10, 20, 21].

Aging, PD, and inflammation have all been shown to inhibit the endogenous response of multipotent stem/progenitor cells (NSCs) isolated from the subventricular region (SVZ) of the brain lateral ventricles [22–24]. Similarly, the neurogenic potential of clonogenic NSCs from the midbrain aqueduct periventricular regions (Aq-PVRs), which are endowed with a specific mDA neuron differentiation potential, is also reduced [25–27]. Overall, age-associated increased mDA neuron vulnerability to insults (oxidative stress and inflammation), dysfunctional neuron–glia crosstalk and impaired neurogenesis represent key contributory factors to the development of PD.

Among all the factors at play within the SNpc microenvironment, we have recently identified a major role for reactive astrocytes and Wnt/ β -catenin signaling in mDA neuronal plasticity and brain repair [25, 28–31]. Reactive astrocytes are key players in the response to injury and inflammation, regulating both helpful and harmful responses [11–17, 32–37]. We have shown that wntless-related MMTV integration site 1 (Wnt1), playing a vital role in the generation of mDA neurons [38–42], is also critically involved in their protection against several neurotoxic/inflammatory insults [28–30] or genetic mutations [39], and regulates SVZ and Aq-PVR plasticity via crosstalk with inflammatory signaling pathways [24, 25, 28–31, 43, 44]. With age, Wnt signaling becomes dysfunctional [24, 25, 28–30, 45–48], with potential consequences for neuron–glia crosstalk, mDA neuron plasticity and repair. These findings are of importance given the deregulation of Wnt signaling in major neurodegenerative diseases including PD [49–56]; and the emerging link between most PD related genes, Wnt signaling and inflammation [43, 44, 54–57].

Current treatments for PD aim at alleviating motor symptoms, but have no effects on the on-going neurodegeneration [58]. As such, the ideal therapeutic regimen for PD should combine both symptomatic treatment and neurorestorative interventions aimed at protecting or enhancing the function of mDA neurons. Evidence exists that NSCs harvested from the adult brain and grafted into laboratory animals with experimental neurodegenerative diseases exert beneficial effects promoting local trophic support and immune modulation, thereby complementing the restorative responses of the endogenous NSC population [59–68]. While the ability of transplanted NSCs to promote beneficial effects in classical preclinical models of PD is increasingly being appreciated [62–68], little is known about the effects of NSC transplants on the aged PD brain.

We performed a carefully constructed time course analysis of the degenerative changes occurring at the nigrostriatal level of aged male mice upon exposure to MPTP, and studied the effects of the unilateral transplantation of syngeneic somatic NSCs within the SNpc. We carried out immunohistochemical and molecular analyses at SNpc, nigrostriatal, and Aq-PVR levels to determine the ability of NSC grafts to ameliorate the host microenvironment and to rescue dysfunctional mDA neurons. We also used *ex vivo* analyses of transgenic β -catenin reporter mice and *in vitro* cell culture paradigms between neurons and glial cells to unravel potential mechanisms underlying the observed effects.

Our data uncover the striking ability of grafted NSCs to reverse age-related nigrostriatal failure to recover of MPTP-lesioned mice and highlight astrocytes and Wnt/ β -catenin signaling as key players in nigrostriatal mDA neurorestoration.

MATERIALS AND METHODS

Mice and Treatments

Aged (16- to 20-month-old) male C57BL/J (Charles River, Calco, Italy) mice were maintained under standard laboratory conditions. All surgeries were performed under anesthesia. The mice received $n = 4$ intraperitoneal (i.p.) injections of vehicle (saline) or MPTP-HCl (Sigma-Aldrich) dissolved in saline, 3 hours apart during 1 day, at a dose of 12 mg/kg^{-1} free base, according to titration studies that produced long-lasting depletion of DA endpoints with no recovery in both striatum (Str) and substantia nigra pars compacta (SNpc) of aged mice without causing toxicity [24, 25, 30]. MPTP was handled in accordance with the reported guidelines [69]. Based on our time course studies [24, 25, 29, 30] and pilot experiments (Supporting Information Methods), a window of 7 days post-MPTP was selected for transplantation of NSCs. The study assessed the SN, the striatum (Str), and the tectal aqueduct (Aq) of the mesencephalon [25–28, 30]. The effects of grafting NSCs in saline-injected mice, or mock cell grafting (ventral midbrain dead cells [VMCs] [65]) in MPTP mice, were also analyzed. Mice were sacrificed at 1, 3, and 7 weeks post-implantation (wpi).

Transplantation of Neural Stem Progenitor Cells

Adult neurospheres were generated from the subventricular zone of 4- to 8-week-old C57Bl/6 as previously described [59–61] and examined further in Supporting Information Methods. NSCs were tagged *in vitro* with lentiviral vectors carrying enhanced green fluorescent protein (GFP). NSCs at passage numbers 8–10 were used. Pilot experiments were conducted for optimization of NSC numbers and timing of NSC transplantation after MPTP (Supporting Information Methods).

On the day of transplantation (i.e., day 7 post-MPTP), MPTP-injected mice exhibiting a significant motor deficit were randomly assigned to MPTP + PBS, MPTP + GFP⁺ NSC grafts, or MPTP + VMCs. Mice were anesthetized with chloral hydrate (600 mg/kg) and positioned in a stereotaxic apparatus. The following stereotaxic coordinates were used: 3.2 posterior to the bregma, 1.5 mm lateral to the midline, and 3.6 mm ventral to the surface of the dura mater. GFP⁺ NSCs or VMCs (100×10^3) were injected unilaterally above the left SN (over a period of 2 minutes). The needle was kept in place for 5 minutes after each infusion before retraction. Mock-grafted controls received the same volume of phosphate buffered saline (PBS). Additionally, a group of control mice treated with saline (instead of MPTP) also received NSC grafts. On the day of sacrifice, mice were given bromodeoxyuridine (BrdU, 50 mg kg^{-1} , injected four times, 2 hours apart) and killed 2 hours after the last injection [24, 31].

Motor Coordination with the Rotarod

The analysis of motor coordination was carried out using an accelerating rotarod (five-lane accelerating rotarod; Ugo

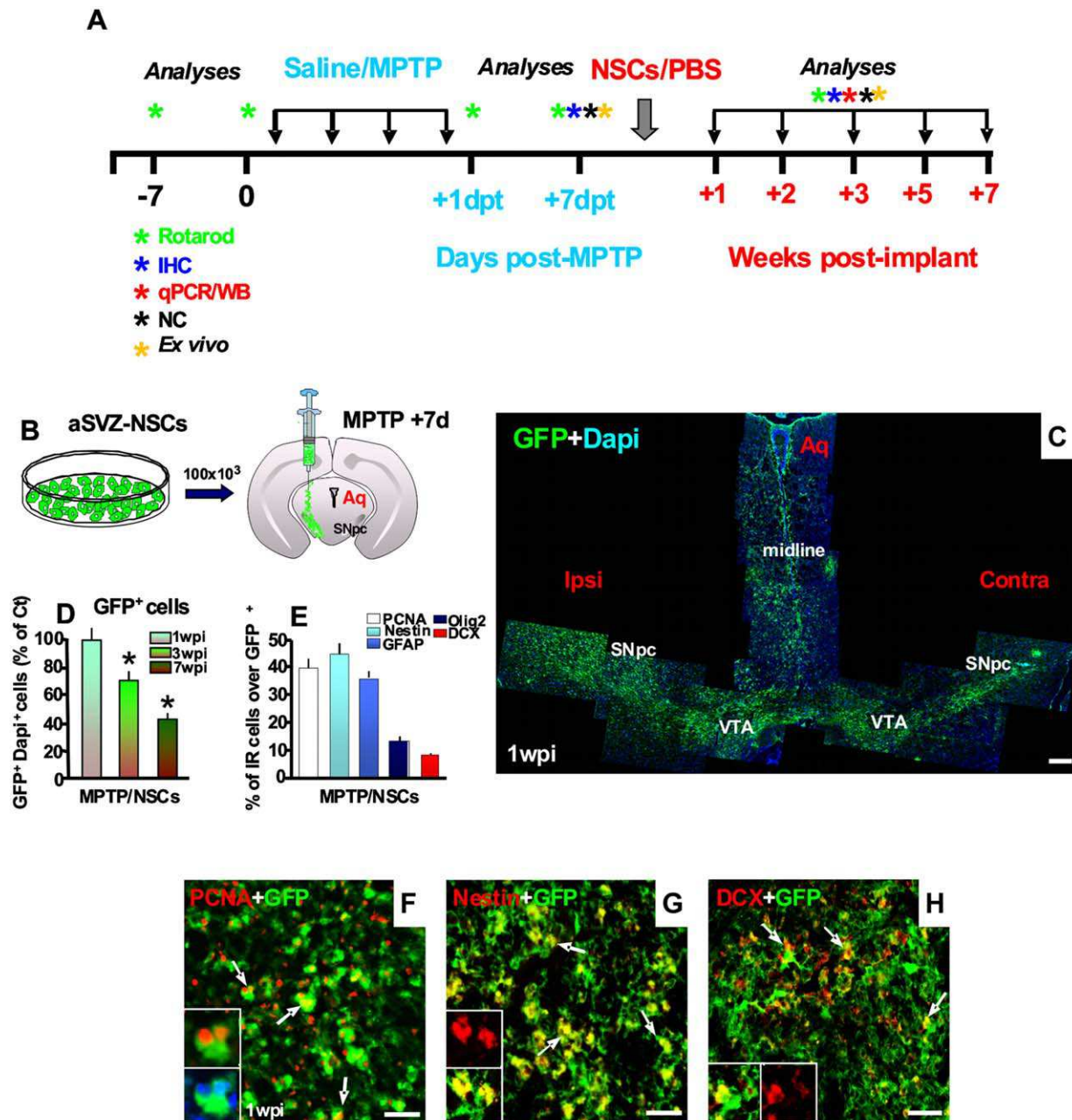


Figure 1. Distribution, proliferation, and fate of NSC grafts. **(A, B)** Schematic representation of the experimental design. Mice treated with MPTP (12 mg kg^{-1} , injected four times) or physiological saline were monitored for their motor behavior with the rotarod (green stars)-MPTP. NSCs or the vehicle (PBS), were unilaterally transplanted above the SNpc, and IHC (blue stars), NC (black stars), qPCR, WB analyses (red stars), or ex vivo studies (orange stars) carried out 1–7 wpi. **(C)** Confocal microscopic image showing robust bilateral engraftment of GFP⁺ NSCs in the SNpc and VTA by 1 wpi. A consistent fraction of GFP⁺ cells distributed to the tegmental aqueduct periventricular regions (Aq-PVRs) and midline. Nuclei were counterstained with Dapi (blue). Scale bar: 400 μm . **(D)** Relative quantification of transplanted NSCs at the SN level. Data (mean \pm SEM, $n = 6$ brain/time point, tp) are percentage of GFP⁺ cells over 1 wpi (100%). **(E)** Quantification of proliferation, glial, or neural differentiation markers by grafted NSCs at 1 wpi. Data (mean \pm SEM) expressed as percentage of IR cells over total GFP⁺ cells. **(F–H)** Grafted GFP⁺ NSCs expressing the proliferation marker, PCNA (E), the neural lineage marker nestin (F) or the marker of neural progenitors, DCX (G) are shown. Magnifications (arrows) are shown in the boxed areas. Scale bars (E–G): 50 μm . *, $p \leq .05$ versus 1 wpi by ANOVA followed by Newman–Keuls test. Abbreviations: Aq, aqueduct; Dapi, 4',6-diamidino-2-phenylindole; DCX, doublecortin; GFP, green fluorescent protein; GFP, green fluorescent protein; IHC, immunohistochemical; IR, immunoreactive; MPTP, 1-methyl-4-phenyl-1,2,3,6-tetrahydropyridine; NC, neurochemical; NSC, neural stem/progenitor cells; PBS, phosphate buffered saline; qPCR, quantitative real-time PCR; SNpc, substantia nigra pars compacta; VTA, ventral tegmental area; WB, Western blot; wpi, weeks post-implant.

Basile, Comerio, Italy), starting 7 days before MPTP treatment and continuing throughout the study [30] (Fig. 1A and Supporting Information Methods). Only MPTP-injected mice exhibiting a

significant decrease in motor performance compared with saline-injected controls were included in the study (Supporting Information Fig. S1).

Immunohistochemistry

On the day of sacrifice, mice were anesthetized and transcardially perfused with 0.9% saline, followed by 4% paraformaldehyde in phosphate buffer (pH 7.2 at 4°C). The brains were carefully removed and processed as previously described [29, 30] and in the Supporting Information Methods. Serial coronal sections (14 μm -thick), encompassing the striatum (Str, 0.74, 0.5, 0.14, and 0.02 mm anterior to the bregma and the SNpc-tegmental Aq (bregma -2.92 to bregma -4.84 mm) were collected, mounted on poly-L-lysine-coated slides, and processed as described (Supporting Information Methods). The preabsorbed primary antibodies used are shown in Supporting Information Table S1 (Supporting Information Methods).

Confocal Laser Scanning Microscopy, Image Analysis, and Quantification of Immunostaining

All the quantifications were performed by investigators blind to treatment conditions. Immunostaining was examined using a Leica LCS-SPE confocal microscope. For fluorescence intensity (FI) assessments and colocalizations, midbrain sections were labeled by immunofluorescence and images were acquired by sequential scanning of 12–16 serial optical sections [24, 25, 29–31]. Three-dimensional reconstructions from z-series were used to verify colocalization in the x - y , y - z , and x - z planes. Serial fluorescent images were captured in randomly selected areas and the number of labeled cells per field ($n = 6$ –8 fields/section) was manually counted in four to six midbrain sections/brain, ($n = 6$ /treatment group) using Olympus cellSense Dimension software, and cell counts obtained averaged (mean \pm SEM) [24, 25, 29–31].

Estimation of Tyrosine Hydroxylase-Positive SNpc Neuron Survival

Tyrosine hydroxylase-positive (TH⁺) SNpc neuronal cell count was determined by serial section analysis of the total number of TH⁺ cells counted throughout the entire rostro-caudal (RC) axis of the murine SNpc (bregma coordinates: -2.92 , -3.08 , -3.16 , -3.20 , -3.40 , and -3.52) according to Franklin and Paxinos [70]. Estimates of total TH- and Nissl-positive (stained with cresyl-violet) neurons in the SNpc adjacent sections were calculated using Abercrombie's correction [25, 29, 30, 71, 72] (Supporting Information Methods) and data expressed as mean \pm SEM ($n = 6$ mice/treatment group/time point, tp).

Determination of Striatal Dopaminergic Endpoints

Striatal TH and dopamine transporter (DAT)-immunoreactive (IR) fiber staining were assessed in $n = 3$ coronal sections at three levels (bregma coordinates: $+0.5$, $+0.86$, and 1.1 mm, respectively), of the caudate-putamen (CPu) in $n = 6$ mice/group/time [30]. Measurements of fluorescence intensity (FI) of TH and DAT staining above a fixed threshold [73] using the corpus callosum for background subtraction were carried out using computer-assisted image analysis software (LEICA), and changes in average FI (mean \pm SD) were expressed as a percentage (%) of saline-injected controls. For high-affinity synaptosomal DA uptake assay to measure the capacity of DA neurons to take up [³H]-labeled DA, left and right striatal homogenates were processed and analyzed as described [25, 29, 30, 74] (Supporting Information Methods).

RNA Extraction, Reverse Transcription, and Real-Time polymerase chain reaction (PCR)

RNA was extracted from tissues/cell samples, as previously detailed [24, 25, 29, 30] (Supporting Information Methods). Briefly, after purification using QIAquick PCR Purification kit (Qiagen), 250 ng of cDNA were used for real-time PCR using predeveloped TaqMan assay reagents (Applied Biosystems). Real-time quantitative PCR was performed using the Step One Detection System (Applied Biosystems) according to the manufacturer's protocol, using the TaqMan Universal PCR master mix (#4304437). The assay IDs are reported in Supporting Information Table S2. For each sample, we designed a duplicate assay and β -actin (Applied Biosystems #4352341E) was used as the housekeeping gene. Quantification of the abundance of target gene expression was determined relative to β -actin with regard to the control group by using the delta C_t ($2^{-\Delta\Delta C_t}$) comparative method, with the results expressed as arbitrary units (AU). Relative-fold changes over saline/PBS or MPTP/PBS are indicated.

Western Blot Analysis

Protein extracts were prepared from tissues from the different treated groups ($n = 6$ mice/treatment group/time-point) and from cell cultures (run in triplicates) within the different experimental groups [24, 25, 29, 30]. The sources and dilutions of the primary antibodies used are detailed in Supporting Information Table S1 and Supporting Information Methods. The bands from the Western blots were densitometrically quantified on x-ray films using ImageQuantity One. Data from experimental bands were normalized to β -actin. Values are expressed as percentage of saline-injected controls. Western blot measurements were repeated $n \geq 4$ times independently.

In Situ Hybridization

In situ hybridization was performed using CY3 AntisenseRNA probes (Sigma Aldrich) specifically for Wnt1, and GAPDH was used as the control probe, as previously described [29, 30]. The sequences of Wnt1 and GAPDH correspond to GeneBank NM 021279 Loc.2106 and NM008084 Loc. 7. Midbrain cryosections (12 μm -thick) at the level of the SNpc were treated, as detailed elsewhere [29, 30].

Glial Cell Cultures and Primary Enriched Neuronal Cultures

For astrocyte derivation from NSCs (N-Astro), the cells were essentially cultured as for primary astroglial cell cultures [24, 25, 29–31, 75, 76] (Supporting Information Methods). The isolated N-Astro (98% of the cells were glial fibrillary acid protein (GFAP)-IR astrocytes) monolayers, were rinsed with sterile PBS and replated with a final density of 0.4 – 0.6×10^5 cells per cm^2 in poly-D-lysine (10 $\mu\text{g}/\text{ml}$)-coated 6-, 12-, or 24-well plates, the conditioned medium (N-ACM) was collected and used as described [76]. Ex vivo isolation and culture of glial cells from either young or aged brain was previously detailed [18, 19, 24, 25, 76–78] (Supporting Information Methods). Isolated young/aged astrocytes (A-Astro, >95 GFAP⁺ cells) and aged microglia (A-Micro, >95 IBA1⁺ cells) were counted and plated at a final density of 0.4 – 0.6×10^5 cells per cm^2 in poly-D-lysine (10 $\mu\text{g}/\text{ml}$)-coated 6-, 12-, or 24-

well plates, and their conditioned media were collected and stored at -70° . Some of the glial cells were exposed to different treatments and processed for qPCR or protein analyses, or were used for direct coculture with primary mesencephalic neurons, as detailed in Supporting Information. For in vitro establishment of primary mesencephalic neuronal cultures, timed pregnant Sprague–Dawley rats (Charles River Breeding Laboratories, Milan Italy) were killed in accordance with the Society for Neuroscience guidelines and Italian law. Primary mesencephalic neurons were prepared from the brain of embryonic day 13–14, as detailed [29, 30] and further processed for coculture with astrocytes according to the different paradigms as described ([29, 30] Supporting Information Methods).

Caspase-3 Activity

Caspase-3 activity was evaluated as cell death marker using the fluorogenic substrate DEVD-AFC (15 μ M in dimethyl sulfoxide; Calbiochem System Products, San Diego, CA), and quantification of DEVD-like fluorescent signal assessed in luminescence-spectrophotometer (excitation 400 nm and emission 505 nm) [29, 30]. Enzymatic activity is expressed as arbitrary fluorescent units (AFUs).

Enzyme-Linked Immunosorbent Assay and NO Production

Levels of cytokines were determined in tissues or cells using enzyme-linked immunosorbent assay (ELISA) kits (DuoSet ELISA Development System; R&D Systems, McKinley Place, MN) following the manufacturer's protocol. NO production was determined by measuring the accumulated levels of stable decomposition product reactive nitrite (RNS) in the culture supernatants with the Griess reagent, corrected for the number of isolated cells afterward [18, 24, 31, 78].

Assessment of Wnt/ β -Catenin Activation/Antagonism In Vivo

To address Wnt/ β -catenin activation, 11- to 16-month-old transgenic (Tg) β -catenin reporter (BATGAL) [25, 79] mice were used. BATGAL express nuclear beta-galactosidase under the control of the beta-catenin-activated transgene (BAT) promoter [79]. The BATGAL reporter mice used in this study were purchased from the Jackson laboratory (Tg(Bat-lacZ)3 Picc/Tg(Bat-lacZ)3Picc) on a C57Bl background. Tg mice were treated with MPTP or saline and after 7 days, NSCs were grafted as described above, whereas control mice received PBS. Aged-matched wild-type (Wt) littermates treated with MPTP were also used as controls. The effect of inhibiting/activating Wnt/ β -catenin signaling was assessed using Dkk1 and Wnt1-Ab (Wnt-Ant) [29], or Wnt1 (Supporting Information Methods). A further control group of mice received the vehicle (PBS) instead of Wnt-Ant. The mice were sacrificed 1, 3, and 5 wpi. Behavioral, spatio-temporal immunohistochemical, and gene expression analyses were carried out as described above.

Data Analysis

Statistical significance between means \pm SEM was assessed using a two-way analysis of variance (ANOVA), and Student's *t* test for paired or unpaired data. Experimental series performed on different days were compared using the Student–

Newman–Keuls *t* test. Values of $p \leq .05$ were considered statistically significant.

RESULTS

Transplanted NSCs Survive and Integrate into the Aged MPTP-Lesioned Host SNpc and Aq-PVR

We first studied the engraftment, proliferation, and distribution of GFP⁺ NSCs that were unilaterally transplanted 7 days post-MPTP in the SNpc of 16- to 20-month-old aged mice (Fig. 1A, 1B).

By 1 week post-implant (wpi), transplanted NSCs were detected both in the ipsilateral and contralateral SNpc (Fig. 1C). A consistent fraction of transplanted NSCs distributed to the tegmental midbrain aqueduct periventricular regions (Aq-PVRs), the region that harbors self-renewing NSCs endowed with dopaminergic (DA) potential [25–27, 30].

At 1 wpi, transplanted NSCs showed robust engraftment at all the SN rostro-caudal levels analyzed, which was followed by a decline at 3 ($71\% \pm 6.2\%$, $p < .05$) and 7 wpi ($42.9\% \pm 4.3\%$, $p < .05$) (Fig. 1D). Quantitative colocalization analyses in midbrain sections at 1 wpi indicated that 40.01% (± 2.8) of engrafted NSCs expressed the proliferative marker PCNA (Fig. 1E, 1F) or BrdU (*not shown*), 44.7% (± 3.8) the cell marker nestin (Fig. 1E, 1G) and 35.9% (± 2.6) the astroglial cell marker GFAP (Fig. 1E), whereas only 13.2% (± 1.6) and 7.9% (± 1.1) of GFP⁺ NSCs were immunoreactive for the oligodendroglial cell marker Olig2⁺ (Fig. 1E) and the neuroblast marker doublecortin (DCX; Fig. 1E, 1H). NSCs transplanted unilaterally in the SNpc of aged mice migrated within the lesioned SNpc of both sides, distributed to the Aq-PVRs and survived up to 7 wpi.

NSC Grafts Promote the Rescue of Endogenous TH⁺ Neurons in the SNpc

The number of dopaminergic neurons in the SNpc was assessed by TH immunoreactivity (Fig. 2A–2E). Stereological quantification of TH⁺ and Nissl⁺ neurons in SNpc was performed to validate TH⁺ neuron survival (Fig. 2F). NSCs grafted into MPTP-lesioned mice (MPTP/NSC) showed a significant ($p \leq .05$) increase in endogenous TH⁺ immunoreactivity and TH⁺ neuron survival at both early (1 wpi) and late (3–7 wpi) time points (Fig. 2A–2C, 2F) versus control MPTP mice treated with PBS (MPTP/PBS; Fig. 2D, 2F). By contrast, grafting NSCs into saline-injected (saline/NSCs) control mice, did not change the number of endogenous TH⁺ neurons, versus saline/PBS mice (Fig. 2F). Additionally, grafting control ventral midbrain dead cells (VMCs) into MPTP mice failed to increase TH⁺ neuron survival (Fig. 2F), which suggests that the observed increase in the number of TH⁺ neuron is lesion- (MPTP injury) and NSC-specific.

The number of TH⁺ neurons in MPTP/NSC mice constantly increased over time and became comparable with unlesioned sham-treated (saline/PBS) control mice at 3 and 7 wpi (Fig. 2E, 2F). The effect of grafted NSCs on TH⁺ neurons was similar in the SNpc ipsilateral and contralateral to the transplantation site (data not shown), and only a few GFP⁺ transplanted cells were found to be immunoreactive for TH (Fig. 2B, 2C, arrows).

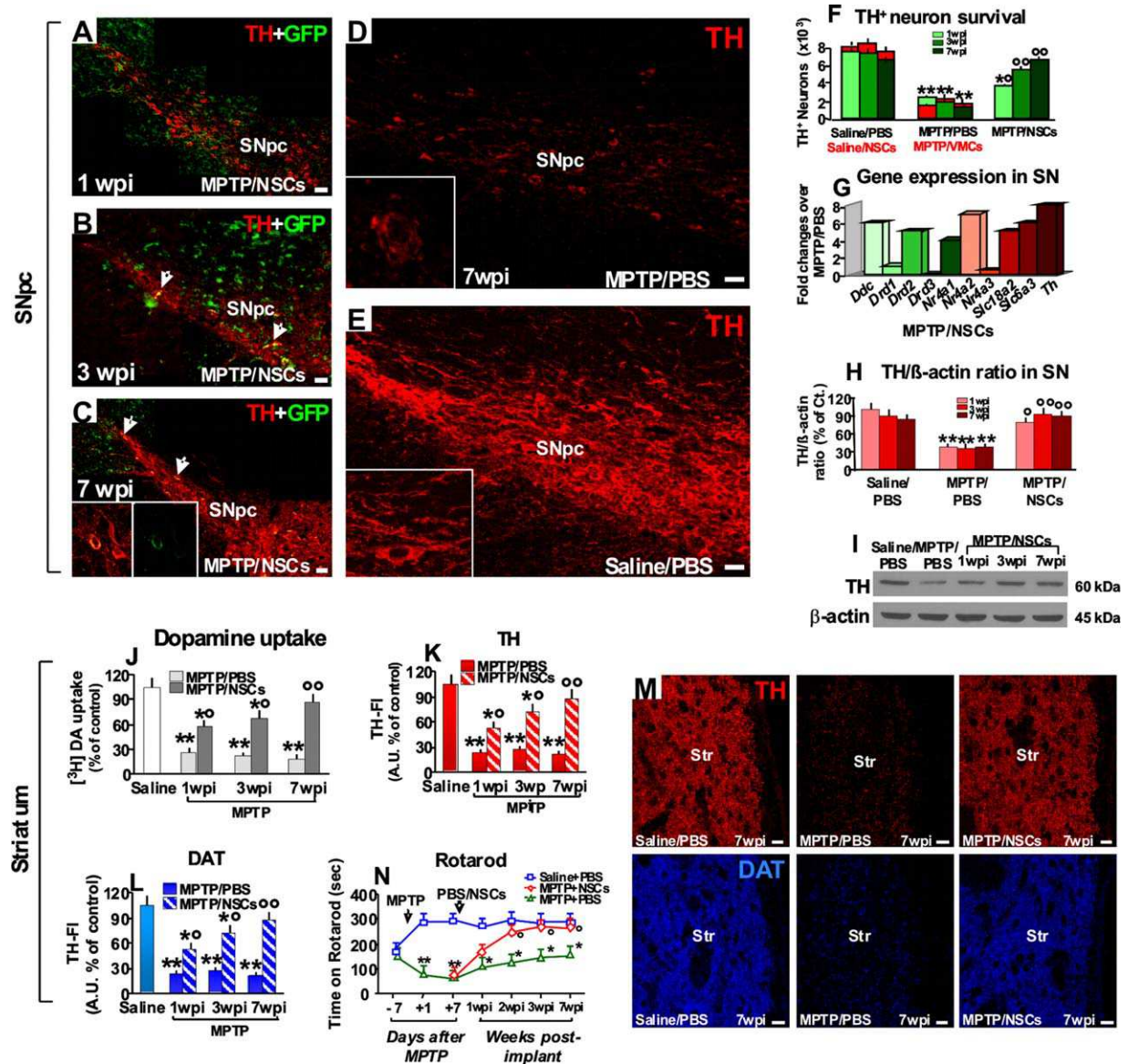


Figure 2. NCS grafts promote survival of endogenous TH⁺ neurons and reverse lifelong nigrostriatal DA toxicity. (A–E): Confocal images of the SNpc in aged (16- to 20-month-old) MPTP-lesioned NCS-grafted mice at 1, 3, and 7 wpi (A–C) compared with aged-matched MPTP/PBS- (D) and saline/PBS- (E) mice at 7 wpi. GFP⁺ and TH⁺ colocalization was only occasionally observed (B and C, arrows). Magnifications (C–E) in the boxed areas. Scale bars: 100 μm. (F): Total number of TH⁺ neurons in the right and left SNpc (mean ± SEM) at 1, 3, and 7 wpi showing that NCS but not VMC (red) grafts increase TH⁺ neuron survival in MPTP mice. NCS grafts had no effect versus saline/PBS mice when transplanted into saline (Saline/NSCs, red) mice. (G): qRT-PCR in SNpc showing 4- to 8-fold upregulation of *AADC*, *Drd2*, *Nr4A2*, *Slc6a3*, *Slc18a2*, and *TH* mRNA of MPTP/NSC over MPTP/PBS values. (H, I): NCS grafts reverse MPTP-induced loss of TH protein by immunoblot (wb) analysis. Data (mean % ± SEM) of TH/β-actin ratio relative to controls. (J): NCS grafts increase high-affinity Str DA uptake assessed by [³H]DA incorporation (mean % ± SEM). (K–M): TH- (K, M) and DAT-FI (L, M), by immunofluorescent staining and image analysis. Scale bars: 20 μm. (N): Motor performances on rotarod showing recovery from motor impairment in MPTP/NSC, but not MPTP/PBS mice. *, *p* ≤ .05; **, *p* ≤ .01, versus saline/PBS; °, *p* ≤ .05; °°, *p* ≤ .01, versus MPTP/PBS, at each time interval, respectively, by ANOVA followed by post hoc Newman–Keuls test. Abbreviations: GFP, green fluorescent protein; MPTP, 1-methyl-4-phenyl-1,2,3,6-tetrahydropyridine; NCS, neural stem/progenitor cells; PBS, phosphate buffered saline; SNpc, substantia nigra pars compacta; Str, striatal; TH, tyrosine hydroxylase; wpi, weeks post-implant.

We applied quantitative real-time PCR (qRT-PCR) of the expression levels of DA-specific mRNA species in MPTP-lesioned SNpc. By 1 wpi, MPTP/NSC mice showed an upregulation (by 4- to 8-fold) of most DA transcripts studied, versus MPTP/PBS control mice (Fig. 2G). These included *Th*, the high-affinity dopamine transporter *Slc6a3* (DAT), the vesicular monoamine transporter *Slc18a2* (VMAT), the DA-specific transcription factor *Nr4a2* (Nurr1) required for the mature DA

phenotype and survival [38, 80], the DA biosynthetic enzyme *Ddc* (DOPA decarboxylase), and the DA receptor subtype 2 *Drd2*. We also found that MPTP/NSC mice showed a significant (*p* ≤ .05) increase in the protein levels of TH as early as 1 wpi, versus MPTP/PBS mice (Fig. 2H, 2I).

Thus, NCS grafts had a significant time-dependent rescue effect on endogenous TH neurons, which occurs at tissue, gene and protein levels. This striking rescue of the MPTP-

induced phenotype, which was bilateral, injury- and NSC-specific, was not attributable to a direct differentiation of transplanted NSCs into TH⁺ neurons, but rather to an as yet unidentified rescue effect on endogenous cells.

NSC Grafts Promote Synaptosomal DA Uptake and DA Innervation in the Striatum, Reverting PD Motor Deficits

To investigate whether NSC grafts increased the functionality of new TH⁺ neurons, we then focused on the striatal targets of the SNpc DA neurons. First, we measured the striatal uptake of radiolabeled DA([³H]-DA) in presynaptic terminals of aged MPTP mice. MPTP/NSC mice showed a significant ($p \leq .05$) recovery of high-affinity striatal synaptosomal DA uptake (vs. MPTP/PBS), as early as 1 wpi (Fig. 2J). This effect in MPTP/NSC mice increased over time, restoring values similar to those of saline/PBS controls by 7 wpi. On the contrary, MPTP/PBS mice showed a constant significant ($p \leq .01$) reduction of synaptosomal DA uptake over time, versus saline/PBS controls.

When we performed quantitative confocal laser microscopy on striatal sections, we found that NSC grafts efficiently counteracted the MPTP-induced loss of striatal TH (Fig. 2K, 2M) and DAT innervation (Fig. 2L, 2M). Conversely, corresponding levels in control MPTP/PBS mice were found to be significantly lower, compared with both MPTP/NSC ($p \leq .05$) and saline/PBS controls ($p \leq .01$) at each time point tested.

Behavior analyses confirmed that these structural and functional striatal changes were coupled by a full and long-lasting recovery of motor coordination deficits in MPTP/NSC mice, versus MPTP/PBS controls, which started to be significant ($p \leq .05$) at 2 wpi (Fig. 2N). Besides the effects of NSC grafts on SNpc-DA neuronal cell bodies, NSCs would promote a progressive recovery of the host striatal DA terminal region function, which further supports their role in enhancing endogenous recovery mechanisms in the aged brain.

NSC Grafts Downregulate the Local Expression of Genes Related to Inflammation and Oxidative Stress While Promoting the Expression of Wnt Signaling and DA Developmental Genes

To further unravel the mechanisms behind the observed structural and functional recovery induced by the NSC grafts, SN tissues from saline/PBS, MPTP/PBS and the entire SN tissues that include the engrafted cells of MPTP/NSCs mice were processed for qPCR analyses and several oxidative stress/inflammatory, Wnt signaling, growth/neurotrophic, and DA-specific developmental mRNA species were analyzed at 1 wpi. We found that the expression levels of various pro-inflammatory mediators involved in inflammation-dependent DA neurotoxicity [11–19] were upregulated 4 to 8-fold in SNpc tissues from MPTP/PBS mice ($p \leq .01$), versus saline/PBS mice (Fig. 3A). In contrast, MPTP/NSC mice showed a significant ($p \leq .01$) downregulation of all these inflammatory mRNA species, including *Tnf* and *Tnfrsf1a*, *Il1*, *Nos2*, *Nfkb*, and the phagocyte oxidase *Cybb* (*gp91phox*), versus MPTP/PBS controls (Fig. 3B).

We next looked at the at the astrocytic *Nrf2-Hmox* axis, which is critically involved in the protection of mDA neurons against cytotoxic stimuli [81]. Importantly, we found that *Nrf2* and *Hmox1* were downregulated by 3- to 4-folds (Fig. 3A) in

SN tissues of MPTP/PBS mice, versus saline/PBS controls ($p \leq .01$), while NSC grafts promoted a significant upregulation ($p \leq .01$) of both genes versus MPTP/PBS mice (Fig. 3B). This finding suggests an ability of NSC grafts to normalize the unbalance of pro-inflammatory and oxidative stress markers in the aged MPTP-lesioned SN milieu.

We also found that the inflammatory chemokines *Ccl3* and *Cxcl11*, which were 4- to 7-fold downregulated in response to MPTP in vivo ($p \leq .01$; vs. saline/PBS mice) (Fig. 3A), underwent significant upregulation in SN tissues of MPTP/NSC mice ($p \leq .01$; vs. MPTP/PBS mice) (Fig. 3B). Interestingly, the endogenous Wnt antagonists (Wnt-ant) *Dkk1*, *sFrp2*, and *Gsk3b* showed marked upregulation of 6- to 14-fold in SN tissues of MPTP/PBS mice, versus saline/PBS controls ($p \leq .01$; Fig. 3C). By contrast, NSC grafts reversed the MPTP-induced upregulation of *Dkk1*, *sFrp2*, and *Gsk3b* in the SNpc compared with MPTP/PBS ($p \leq .01$; Fig. 3D). As a result, NSC grafts significantly upregulated most key elements of the canonical Wnt/ β -catenin signaling pathway, including *Wnt1*, its transcriptional activator, *Ctnnb1* (β -catenin), and the receptors *Fzd1* and *Fzd2*, as opposed to SNpc tissues from MPTP/PBS mice, which showed a 4- to 7-fold downregulation ($p \leq .01$) versus saline/PBS controls (Fig. 3C, 3D). MPTP/NSC mice showed no changes in *Wnt3a* levels, while *Wnt5a* was upregulated (≥ 4 -fold), versus MPTP/PBS mice (Fig. 3D).

NSC grafts did not change the mRNA levels for a number of growth and neurotrophic factors, including *Egfr*, *Gdnf*, *Igf1*, *Ngf*, *Tgfb*, and *Fgf8* (Fig. 3E). By contrast, several DA-specific developmental factors, including *En1/En2*, and the direct Wnt1/ β -catenin signaling targets, *Lef1*, *Lmx1a*, and *Fgf20*, as well as the indirect Wnt1/ β -catenin targets *Pitx3* and *Bdnf* [38, 39, 82–84], were upregulated by about 2.5- to 3.5-fold ($p \leq .01$) in MPTP/NSCs, versus MPTP/PBS, with *Wnt1* being the most upregulated factor amongst those studied ($p \leq .01$ vs. all mRNAs; Fig. 3E).

The importance of Wnt1 in the response to MPTP was further confirmed at 1, 3 and 7 wpi by WB and gene expression analysis (Fig. 3E–3G). This effect in MPTP/NSC mice was coupled with a robust upregulation of the protein expression of β -catenin and Fzd-1 in the SNpc at all time intervals studied ($p \leq .01$, vs. MPTP/PBS mice; Fig. 3F, 3H). These gene and protein expression profiling data suggest that NSC grafts induce major changes in several inflammatory and Wnt/ β -catenin-dependent genes within the SN of aged MPTP mice.

NSC Grafts Increase Astrocytic Response and Wnt Signaling in Aged MPTP-Lesioned SNpc and Aq-PVRs

Astrocytes represent a vital source of neurotrophic and immune regulatory factors playing critical roles for mDA neuron survival and/or vulnerability [32–37, 76, 85–88]. We then focused our attention on the characterization of the astroglial response after MPTP injury and the effects of NSC transplantation. We found that the number of GFAP⁺/(4',6-diamidino-2-phenylindole (Dapi⁺)) (Vector Laboratory, Burlingame, CA) and S100 β ⁺/Dapi⁺ astrocytes in the SNpc of control MPTP/PBS mice was significantly ($p \leq .01$) increased (1.8- to 2.5-fold) as a result of MPTP injury per se (GFAP/Dapi⁺ [255.6% \pm 24.9%; 226.5% \pm 20.5% and 202.9% \pm 17.5%, vs. saline/PBS mice for GFAP at 1, 3 and 7 wpi, respectively] and S100 β /Dapi⁺ cells [201% \pm 21.5%; 220.6% \pm 17.2%; and 190% \pm 21.5%, vs. saline/PBS, at 1, 3 and 7 wpi, respectively]), (Fig. 4A, 4B).

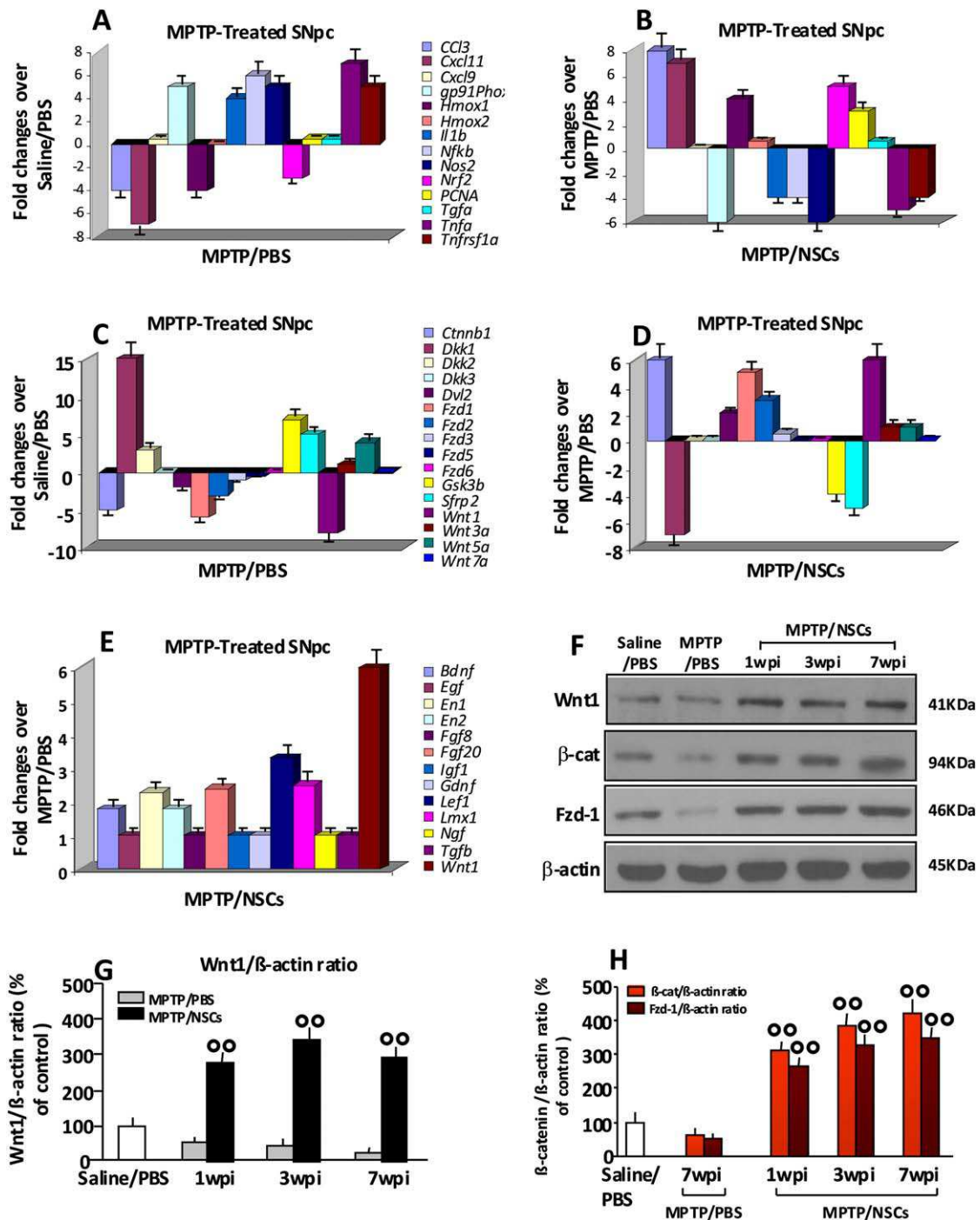


Figure 3. NCS grafts regulation of mRNAs related to inflammation, oxidative stress, Wnt signaling, and dopaminergic neurodevelopment. SNpc tissues were processed for gene expression analyses of mRNA species using qRT-PCR. (A, B): in MPTP/PBS, inflammatory/oxidative stress (*Tnf* and *Tnfrsf1a*, *Il1*, *Nos2*, *Nfkb*, and *gp91phox*) mRNAs are all upregulated by 4- to 8-fold ($p \leq .01$) versus saline/PBS mice (A), as opposed to MPTP/NSC mice showing significant ($p \leq .01$) downregulations versus MPTP/PBS (B). By contrast, NSC grafts upregulated *Nrf2*, *Hmox1*, *CCL3*, and *Cxcl11* (B) ($p \leq .01$) by 4- to 8-fold versus MPTP-PBS (A). (C, D): The Wnt-ant, *Dkk1*, *sFrp2*, and *Gsk3b* were upregulated by 6- to 14-fold in MPTP/PBS versus saline/PBS ($p \leq .01$), whereas NSC grafts reverse MPTP-induced upregulation of *Dkk1*, *sFrp2*, and *Gsk3b* ($p \leq .01$ vs. MPTP/PBS) and significantly upregulate *Wnt1*, *Ctnnb1*, *Fzd1*, and *Fzd2*, ($p \leq .01$ vs. MPTP/PBS) (D). (E): Within the neurotrophic and developmental factors, NSC grafts did not change the mRNA levels of *Egf*, *Gdnf*, *Fgf8*, *Igf1*, *Ngf*, and *Tgfb*, whereas the direct (*Fgf20*, *Lef1*, *Lmx1a*), and indirect (*Bdnf*, *Pitx3*) Wnt1/ β -catenin signaling targets, in addition to the *En1/En2* genes, were upregulated by about 2.0- to 3-fold ($p \leq .01$) in MPTP/NSC versus MPTP/PBS, albeit *Wnt1* was the most frequently upregulated ($p \leq .01$ vs. all factors examined). (F-H): Temporal changes of *Wnt1* mRNA by qRT-PCR (C, arbitrary units, AU) and WB of *Wnt1*, β -catenin, and *Fzd-1* (F, G) showing a significant upregulation in MPTP/NSC mice versus MPTP/PBS mice (E-H). $^{\circ\circ}$, $p \leq .01$, versus MPTP/PBS, at each time interval respectively, by ANOVA with post hoc Newman-Keuls. Abbreviations: MPTP, 1-methyl-4-phenyl-1,2,3,6-tetrahydropyridine; NSC, neural stem/progenitor cells; PBS, phosphate buffered saline; SNpc, substantia nigra pars compacta; wpi, weeks post-implant.

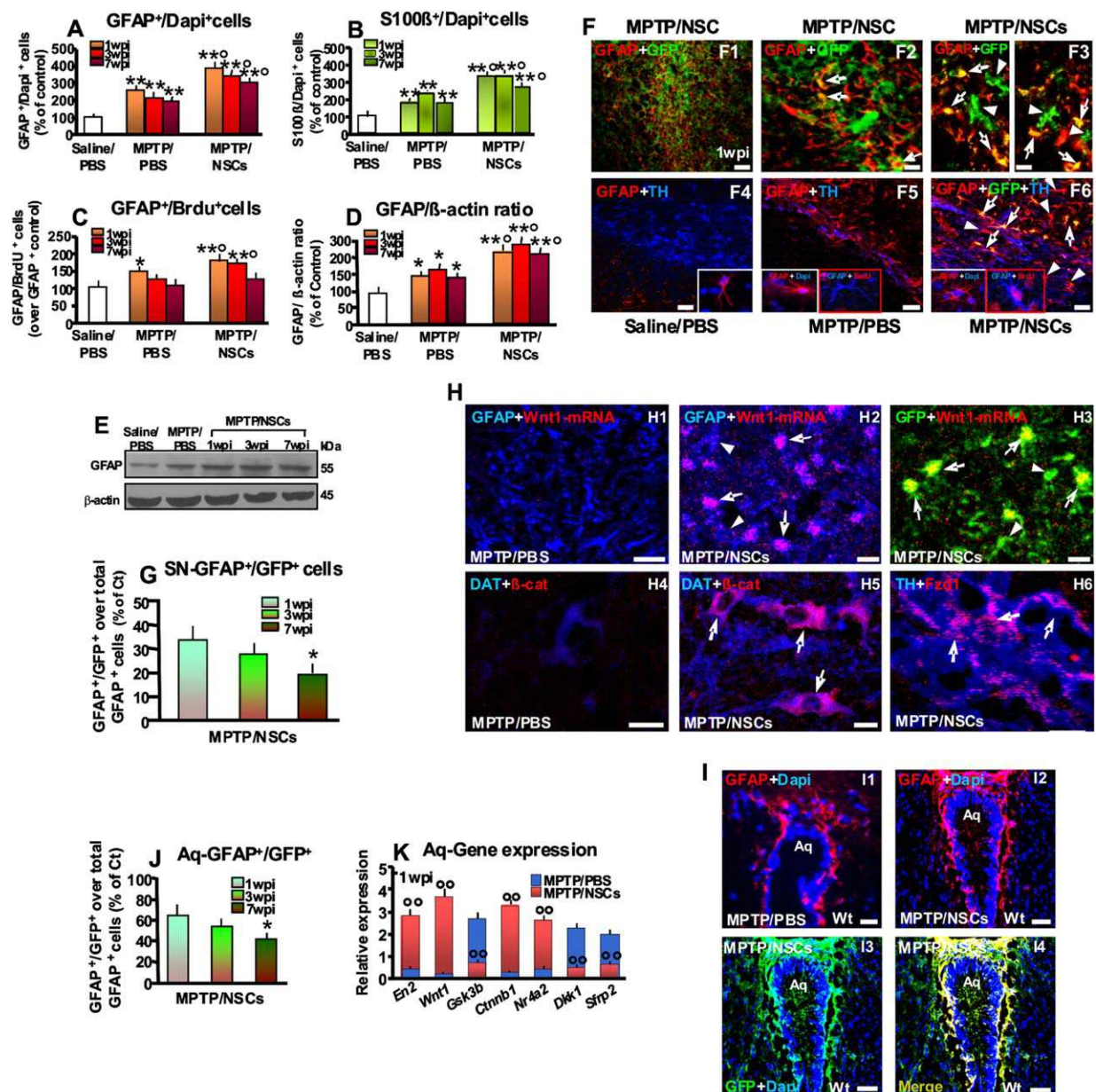


Figure 4. NSC grafts increase the astroglial response and Wnt signaling in aged MPTP-lesioned SNpc and Aq-PVRs. (A–E): NSC grafts increased astrocyte cell number [GFAP⁺/Dapi⁺ (A), S100β⁺/Dapi⁺ (B)], proliferation [GFAP⁺/BrdU⁺ (C)] and GFAP expression (D–E) over MPTP/PBS within the SNpc. (F): Endogenous GFAP⁺ (red) GFP⁺ astrocytes (en-Astro, arrowhead) are in close contact with GFAP⁺(GFP⁺) exogenous NSC-derived astrocytes (ex-Astro, orange–yellow, arrows) (F1–F3), and both cell types in close juxtaposition to TH⁺ (blue) neurons (F6). Scale bars: F1, 200 μm; F2, F3, 40 μm; F4–F6: 100 μm. (G): GFAP⁺/GFP⁺ cells represented only a minority of the total number of GFAP⁺ astrocytes as quantified at 1–7 wpi in SNpc. (H): NSC grafts increased *Wnt1* (red) expression in both en-Astro (blue, H2) and ex-Astro (green, H3) by in situ hybridization histochemistry coupled to immunofluorescence. *Wnt1* was not detected MPTP/PBS en-Astro (H1). NSC grafts increase β-catenin (red) and DAT (blue), TH (blue) and Fzd-1 (red) expression in SNpc DA neurons versus MPTP/PBS (H4–H6). (I, J): NSC grafts increased GFAP⁺ cells (red) (I1–I2) colocalizing with GFP (I3–I4) at the level of the Aq-PVRs, where a vast proportion of GFAP⁺GFP⁺ double labeled cells were counted (J) throughout the study. (K): NSC grafts upregulated *Wnt1*, *Ctnnb1*, *En2*, and *Nr4a2*, whereas *Dkk1*, *sFrp2*, and *Gsk3b* are downregulated versus MPTP/PBS by qRT-PCR analysis in Aq-PVR tissues at 1 wpi. *, $p \leq .05$; **, $p \leq .01$, versus saline/PBS; °, $p \leq .05$; °°, $p \leq .01$, versus MPTP/PBS, at each time-interval; in (E) and (H) *, $P \leq .05$ versus 1 wpi. Abbreviations: Dapi, 4',6-diamidino-2-phenylindole; MPTP, 1-methyl-4-phenyl-1,2,3,6-tetrahydropyridine; NSC, neural stem/progenitor cells; PBS, phosphate buffered saline; wpi, weeks post-implant; Wt, wild-type.

The transplantation of NSCs, but not of VMCs (*data not shown*), further boosted this response, leading to a significant ($p \leq .05$) increase (3- to 3.9-fold) of GFAP⁺ astrocytes versus MPTP/PBS mice at all time-points studied (396.8% ± 48.7%, 345.3% ± 42.4%, and 309.1% ± 37.1% at 1, 3, and 7 wpi, respectively). Likewise, grafted NSCs further increased S100β/

Dapi⁺ cells throughout the study, versus MPTP/PBS mice (326.5% ± 27.6%, 334.3% ± 28.4%, and 292.3% ± 29.4%, at 1, 3 and 7 wpi, respectively; Fig. 4B).

Double staining with BrdU and GFAP showed a significant ($p \leq .05$) increase in GFAP⁺/BrdU⁺ double positive cells over the total number of GFAP⁺ cells after MPTP injury, lasting for

1 wpi ($151.2\% \pm 14.7\%$, $130.2\% \pm 19.2\%$, and $104.6\% \pm 12.0\%$, at 1, 3, and 7 wpi, respectively; Fig. 4C). NSC—but not VMC—grafts further increased GFAP⁺/BrdU⁺ cells ($186.2\% \pm 24\%$, $180\% \pm 19.5\%$, and $120\% \pm 16.7\%$, at 1, 3, and 7 wpi, respectively), versus saline/PBS at all times tested ($p \leq .01$), and versus MPTP/PBS ($p \leq .05$) at 1 and 3 wpi respectively, which indicated some endogenous astroglial proliferation promoted by NSC grafts (Fig. 4C). We found that the protein expression levels of GFAP displayed similar behavior with a significant increase in the SNpc of MPTP/NSC mice versus MPTP/PBS controls ($p \leq .05$) at all time points tested (Fig. 4D, 4E).

We also performed a quantitative confocal analysis of endogenous GFAP⁺/GFP⁻ astrocytes (En-Astros) and exogenous GFAP⁺/GFP⁺ NSC-derived astrocytes (ex-Astros) (Fig. 4F, 4G). En-Astros accumulated in close contact with ex-Astros (Fig. 4F1–4F3), and both cell types were found in close juxtaposition to TH⁺ neurons (Fig. 4F6). However, ex-Astro represented only a minority of the total number of GFAP⁺ astrocytes ($33.4\% \pm 6\%$) at 1 wpi, with their numbers further decreasing over time ($27.2\% \pm 5\%$ and $19.2\% \pm 3.8\%$ at 3 and 7 wpi, respectively; Fig. 4G).

We next speculated that grafted NSCs might influence Wnt signaling within the aged MPTP-injured SN. In situ hybridization histochemistry of Wnt1 coupled with immunofluorescent staining with GFAP or GFP showed that Wnt1 was expressed in both en-Astro and ex-Astro in the SNpc of MPTP/NSC mice (Fig. 4H2, 4H3). Given this increase of Wnt1 in astrocytes we further studied the key elements of the canonical Wnt signaling pathway, Fzd-1 and its transcriptional activator, β -catenin, in SNpc-DA neurons and found that DAT⁺/TH⁺ neurons within the SNpc of MPTP/NSC mice increased the expression of β -catenin (Fig. 4H5) and Fzd-1 (Fig. 4H6) versus MPTP/PBS mice (Fig. 4H4).

Given the preferential distribution of grafted cells to the Aq-PVRs that harbors self-renewing NSCs endowed with dopaminergic (DA) potential [25–27, 30], we next addressed whether NSC grafts might influence the aging-induced inhibition of Wnt signaling in the Aq-PVR-DA niche [25]. We found that GFAP⁺ cells in the Aq-PVRs were increased in MPTP/NSC mice (Fig. 4I1, 4I2), with $65.5\% (\pm 6.5)$, $54.8\% (\pm 5.3)$, and $41.7\% (\pm 3.6)$ of the total number of GFAP⁺ astroglial cells also being GFP⁺ at 1, 3, and 7 wpi, respectively, (Fig. 4I3, 4I4, 4I). Importantly, these GFP⁺/GFAP⁺ cells were seen bordering the ventricular wall all along the Aq-PVRs and the Aq-tail, delineating a thick layer of Dapi⁺ GFP⁻/GFAP⁻ cells, mirroring the localization of GFAP⁺ cells observed in young MPTP-treated mice exhibiting a robust DA neurorestoration [25]. By contrast, aged MPTP mice showed only a slight increase GFAP⁺ cells (Fig. 4I1), supporting an impairment of the aged Aq-PVR GFAP response to MPTP injury [25]. Quantitative RT-PCR analyses of Wnt signaling transcripts in Aq-PVRs tissues at 1 wpi showed that NSC grafts significantly ($p \leq .01$) upregulated Wnt1, Ctnnb1, and the DA-specific developmental transcripts En2 and Nr4a2 [38–41], versus MPTP/PBS mice (Fig. 4K). Consistently, NSC grafts downregulated the expression of Wnt-ant transcripts, including Dkk1, sFrp2, and Gsk3b ($p \leq .01$), versus MPTP/PBS mice (Fig. 4K).

These data suggest that grafted NSCs induce an increase in the overall astroglial response within the MPTP-lesioned brain, partially via direct differentiation, but more consistently

via an increase in endogenous GFAP⁺ astrocytes. NSC grafts in the aged SNpc trigger the expression of Wnt1 in endogenous astrocytes, and Fzd-1/ β -catenin expression in SNpc-TH⁺/DAT⁺ neurons. Additionally NSC grafts promote the accumulation of GFP⁺/GFAP⁺ cells and increase Wnt signaling in the Aq-PVR niche accompanying the upregulation of several mDA-specific developmental genes.

NSC Graft-Derived Astrocytes and NSC-Treated Astrocytes Reverse MPP⁺-Induced Neuronal Death In Vitro: Involvement of Wnt/ β -Catenin Signaling

We then hypothesized that NSC grafts might be associated with an increased Wnt-dependent response in astrocytes, which contributed to supporting TH neuronal survival in the MPTP-lesioned SN [25, 28–30]. To test this hypothesis, we adopted two in vitro reductionist approaches aimed at assessing the protective effects of astrocytes derived from NSCs, and the effects of NSC treatment on endogenous aged astrocytes (Fig. 5A–5I).

We first isolated primary mesencephalic DA neurons and exposed them to MPP⁺ upon coculture with either NSC-derived astrocytes (N-Astros) or N-Astro-conditioned media (N-ACM; Fig. 5A). We found that coculture with N-Astros (Fig. 5B4, 5B5), or direct exposure to N-ACM (Fig. 5B7, 5B8), induced a significant increase in TH⁺ neuron survival (Fig. 5C), DA uptake levels (Fig. 5D), while reducing Caspase3 activity (Fig. 5E), in the absence or the presence of MPP⁺ cytotoxic challenge. By contrast, treatment of TH⁺ neurons with the conditioned media of NSCs (N-CM, containing 0% GFAP⁺ astrocytes) failed to exert any protective effects against MPP⁺ toxicity (*data not shown*).

Interestingly, the exposure of N-Astro-TH neuron cocultures or N-ACM-treated TH⁺ neurons to different Wnt/ β -catenin antagonist (Dkk1, sFrp2, Fzd-CRD or Wnt1-Ab, Wnt-ant) efficiently counteracted the beneficial effects of N-Astro and N-ACM against Mpp⁺ toxicity (Fig. 5B6, 5B9, 5C–5E). On the contrary, the exposure of TH⁺ neurons cultured in the absence of astrocytes (alone) to Wnt-ant had no effect on either TH⁺ neuron survival and DA uptake levels, nor Caspase3 activity (Fig. 5C–5E). Finally, the exposure of TH⁺ neurons to Wnt1 before the MPP⁺ challenge efficiently counteracted MPP⁺-induced inhibition of TH⁺ neuron survival and DA uptake levels, while decreasing Caspase3 activity (Fig. 5B3, 5C–5E). These results confirm the direct effect of Wnt1-mediated signaling from NSC-derived astrocytes on TH⁺ neuroprotection.

To investigate whether NSCs might have an effect on Wnt signaling of endogenous aged (A-Astro) compared with young (Y-Astro) astrocytes (Fig. 5F–5I), primary mesencephalic DA neurons were exposed to MPP⁺ upon coculture with Y-Astro (2 M) or A-Astro (16 M) that were subjected to different pretreatments as it follows. To mimic the conditions of the MPTP-injured microenvironment, Y-Astro and A-Astro were pretreated with either TNF- α + IL-1 β (the two cytokines found to be most downregulated by NSC grafts in vivo), or CCL3 + CXCL11 (the two chemokines found to be most upregulated by NSC grafts in vivo), or conditioned media from aged microglia (A-MCM), or conditioned media of NSC (N-CM). After 24 hours of pretreatment, Y-Astro and A-Astro were washed in PBS and then seeded in the top TH⁺ neurons.

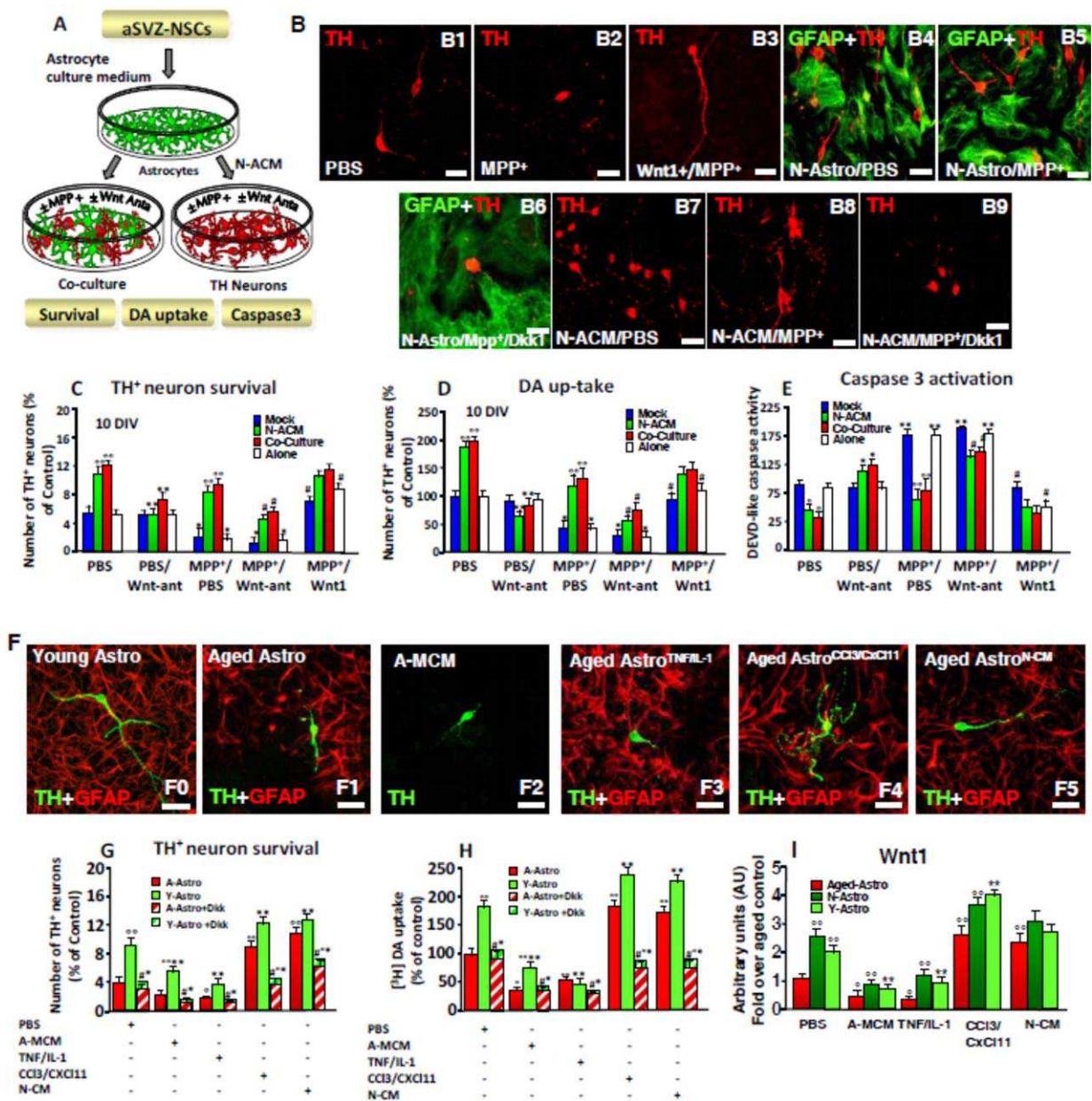


Figure 5. NSC graft-derived astrocytes and NSC-treated astrocytes reverse MPP⁺-induced neuronal death in vitro: involvement of Wnt/ β -catenin signaling. **(A)** Scheme of aSVZ-NSC derivation of astrocytes (N-astro) and direct (coculture) and indirect (N-astro conditioned medium, N-ACM) culture paradigms with primary mesencephalic DA neurons. **(B)** Confocal images of TH⁺ (red) neurons cultured alone in the absence (B1) or presence of MPP⁺ without (B2) or with a Wnt1 pre-treatment (B3); in coculture with N-Astro (B4–B6); or in the presence of N-ACM without (B7–B8) or with (B9) Dkk1. Bars, 20 μ m. **(C–E)** Quantification of TH⁺ neurons at 10 DIV (C); DA uptake levels measured by [3H]DA incorporation (D); and Caspase3-like activity detected with the fluorogenic substrate DEVD-AFC (E). A nonspecific (mock) cell preparation was used as a control. Mean \pm SEM values ($n = 3$ different culture preparations) are reported. $^{\circ}$, $p \leq .01$ versus mock, *, $p \leq .05$; **, $p \leq .01$ versus PBS; #, $p \leq .05$ versus MPP⁺, within each group, respectively. **(F)** Confocal images of TH⁺ (green) neurons cocultured with young (F0) or with aged astrocytes (F1, red) in the direct (F1, F3–F5) or indirect (F2) paradigm, in the presence of A-MCM, TNF- α + IL-1 β (F1, F3), CCl3 + CxCl11 (F4), or N-CM pretreatments (F5). **(G–I)** TH neuron survival (G), DA up-take levels (H), and qRT-PCR of Wnt1 (I). Dkk effect in Aged (dashed-red) versus Young (dashed-green) is shown. $^{\circ}$, $p \leq .05$; $^{\circ\circ}$, $p \leq .01$ versus aged-astro PBS; *, $p \leq .05$; **, $p \leq .01$ versus young-astro PBS; #, $p \leq .05$ versus without Wnt-ant, by ANOVA followed by the Newman–Keuls test. Abbreviations: A-MCM, aged microglia conditioned media; DA, dopaminergic; NSC, neural stem/progenitor cells; PBS, phosphate buffered saline; SVZ, subventricular region; TH, tyrosine hydroxylase.

Cocultures with A-Astro induced an inhibition of TH⁺ neuron survival and a decrease of DA uptake levels compared with coculture with Y-Astro, which promoted instead a significant ($p \leq .01$) increase in TH⁺ neuron survival and functionality (Fig. 5F0–5F1, 5G, 5H). Y-Astro pretreated with TNF-

α + IL-1 β or A-MCM significantly decreased both TH⁺ neuron survival and DA uptake levels (Fig. 5G, 5H). A-Astro pretreated with TNF- α + IL-1 β or A-MCM had a further worsening effect on both parameters, compared with either Y-Astro, or A-Astro without pretreatment (Fig. 5F2, 5F3, 5G, 5H). On the contrary,

A-Astro pre-treated with CCL3 + CXCL11 or N-CM efficiently counteracted the MPP⁺-induced reduction of TH neuron survival and DA uptake (Fig. 5F4, 5F5, 5G, 5H). Pretreatment of neurons with Wnt-ant inhibited these effects (Fig. 5G, 5H), thus suggesting that astrocyte-derived Wnt1/ β -catenin signaling contributed to the observed TH neuroprotection.

Next, we found that the basal Wnt1 expression was significantly decreased in A-Astro compared with either Y-Astro or N-Astro (Fig. 5I). Moreover, pretreatment of Y-Astro and N-Astro with A-MCM or TNF- α + IL-1 β , significantly downregulated Wnt1 expression and further decreased Wnt1 expression in A-Astro (Fig. 5I). On the contrary, Y-Astro, N-Astro, or A-Astro pretreatment with CCL3 + CXCL11 or the CM of NSCs, promoted a significant upregulation of Wnt1 expression (Fig. 5I), supporting Wnt1 as potential mediator of the graft-mediated neurotrophic and functional effects.

During aging and inflammatory conditions, endogenous astrocytes might reduce Wnt1 expression losing their neuroprotective functions against MPP⁺. NSCs counteract this mechanism via direct differentiation in Wnt-competent astrocytes and via the promotion of Wnt signaling in endogenous astrocytes.

NSC Grafts Reduce the Microglial Pro-Inflammatory Status In Vivo and Reverse MPP⁺-Induced Microglial Inflammatory Mediators In Vitro

With age, microglial cells become “primed,” that is, capable of producing exacerbated levels of proinflammatory cytokines and inducible nitric oxide synthase (iNOS)-derived NO when challenged with inflammatory/neurotoxic stimuli [11–19, 89–91]. We then questioned whether NSC grafts might have a direct effect on microglial responses and cytokine secretion. We first acutely isolated microglial cells from MPTP-injured mice *ex vivo*. We found that microglia from MPTP/NSC mice displayed a significant reduction in the mRNA expression of *Il1*, *Tnf*, *Nos2*, and *gp91phox* ($p \leq .01$) and a concomitant upregulation ($p \leq .01$) of *Ccl3*, versus MPTP/PBS mice and saline/PBS mice (Fig. 6A). This effect was associated with a significant decrease in TNF- α , IL-1 β , and iNOS-derived reactive nitrite species (RNS) in supernatants of microglial cells isolated from MPTP/NSC ($p \leq .01$), versus MPTP/PBS mice (Fig. 6B). When we examined the microglial cell number and phenotype *in vivo*, we found that NSC grafts promoted a significant ($p \leq .01$) reversal of IBA1⁺ microglial cells displaying the morphology of activated amoeboid microglia [92, 93] (152.8% \pm 15.2% at 1 wpi, 143.5% \pm 13.1%, at 3 wpi, and 139.1% \pm 10.8% by 7 wpi), versus MPTP/PBS mice (Fig. 6C, 6D). These data suggest that NSC grafts might efficiently override the microglial pro-inflammatory status and reduce the number of IBA1⁺ cells within the aged MPTP-lesioned SNpc.

Given the emerging role of Wnt signaling in the inflammatory response [43, 44, 89, 92–96], we next used *ex vivo* cultures of microglia from young and aged rodent brain [18, 19], to address the immunomodulatory effects of NSC-derived astrocytes (N-ACM) and Wnt signaling on pro-inflammatory mediators of young (Y-micro) versus aged (A-micro) microglial cells, *in vitro*. A-micro challenged with MPP⁺ upregulated RNS, TNF- α , and IL-1 β , at higher levels compared with Y-micro (Fig. 6G, 6H). A-micro also increased GSK-3 β , while reducing β -catenin expression (Fig. 6I, 6J), versus with Y-micro (*data not shown*).

When both Y- and A-micro were pretreated with either N-ACM, recombinant Wnt1, or the specific GSK-3 β antagonist AR (conditions “Wnt-on”), we found significant ($p \leq .05$) inhibition of TNF- α , IL-1 β , and RNS, with higher ($p \leq .05$) inhibition observed in Y- versus A-microglial cultures (Fig. 6G). This effect was associated with a significant ($p \leq .05$) upregulation of β -catenin in the face of a strong inhibition of GSK-3 β expression (Fig. 6I, 6J). On the contrary, when Y- or A-micro were pretreated with Wnt antagonists Wnt1-Ab or Dkk1 (conditions “Wnt off”), upregulated levels of TNF- α , IL-1 β , and RNS were observed (Fig. 6H), suggesting that Wnt/ β -catenin signaling activation is required to downmodulate age and MPP⁺-induced exacerbated levels of glial proinflammatory mediators. These data show an age-dependent exacerbation of pro-inflammatory mediators in MPP⁺-challenged microglia, which suggests that NSC-derived astrocytes and Wnt/ β -catenin signaling activation reverse MPP⁺-induced upregulation of inflammatory markers.

Wnt/ β -Catenin Signaling Antagonism Counteracts the Therapeutic Effects of NSC Grafts on the SNpc and Aq-PVRs of MPTP Mice

To further substantiate the role of Wnt signaling for the therapeutic effects of NSC grafts, we finally investigated whether a “Wnt1-off” condition would abolish the observed NSC graft-induced increased TH⁺ neuron survival and immunomodulation; as well as whether a “Wnt1-on” setting would counteract MPTP-induced SNpc-neuron loss (Fig. 7A–7S, Supporting Information Fig. S3). As such, the following treatment groups were studied: saline/PBS; MPTP/PBS; saline/Wnt-Ant; MPTP/Wnt-Ant; MPTP/Wnt1; MPTP/NSCs; MPTP/NSCs/Wnt-Ant.

Wnt-Ant treatment (either Dkk1 or Wnt1-Ab) of aged mice treated with saline significantly ($p \leq .01$) reduced TH⁺ neuron survival (by about 40%) (Fig. 7B). Wnt-Ant treatment of MPTP-injured mice, which already expressed high levels of endogenous Dkk1 (Fig. 3B), did not further decrease the already low TH⁺ neuron numbers ($\leq 70\%$) (Fig. 7B). Most importantly, Wnt/Ant treatment of MPTP/NSCs mice efficiently reversed the NSC graft-induced increased TH⁺ neuron survival (Fig. 7B). Specifically, Wnt-Ant inhibitory effect was observed at all time intervals tested after NSC grafting (1–5 wpi) (Supporting Information Fig. S3A, S3B). Treatment of MPTP mice with Wnt1 instead led to a significant ($p \leq .01$) degree of protection against MPTP-induced TH⁺ neuron loss (Fig. 7B).

MPTP/NSC grafts also promoted a progressive increase in the number of Nurr1⁺/TH⁺ neurons (Fig. 7C, 7E) and β -catenin⁺/DAT⁺ neurons (Fig. 7D) out of the total number of Nurr1⁺ and DAT⁺ neurons, respectively. Instead, in MPTP/NSCs treated with Wnt-Ant, Nurr1⁺/TH⁺, and β -catenin⁺/DAT⁺ neurons were sharply reduced to levels comparable with those determined in MPTP/PBS mice (Fig. 7C, 7D, 7F). Together, these findings support Wnt/ β -catenin activation as a critical signal for the survival of mDA neurons [29, 30, 39, 49–53], and for NSC graft-induced TH neurorestoration.

We next investigated the effect of Wnt-Ant on astroglial and microglial cells of MPTP/NSCs mice. We found that GFAP⁺ cell density was reduced in MPTP/NSC mice treated with Dkk1 versus MPTP/NSC mice (Fig. 7L–7M). We also found that Wnt-Ant counteracted the effect of the NSC graft on IBA1⁺ microglia. Dual immunostaining with IBA1 and TH confirmed that the inhibitory effect of NSC graft on IBA1⁺ cells (Fig. 7H, 7K) was significantly abolished by Dkk1 treatment (Fig. 7I, 7K).

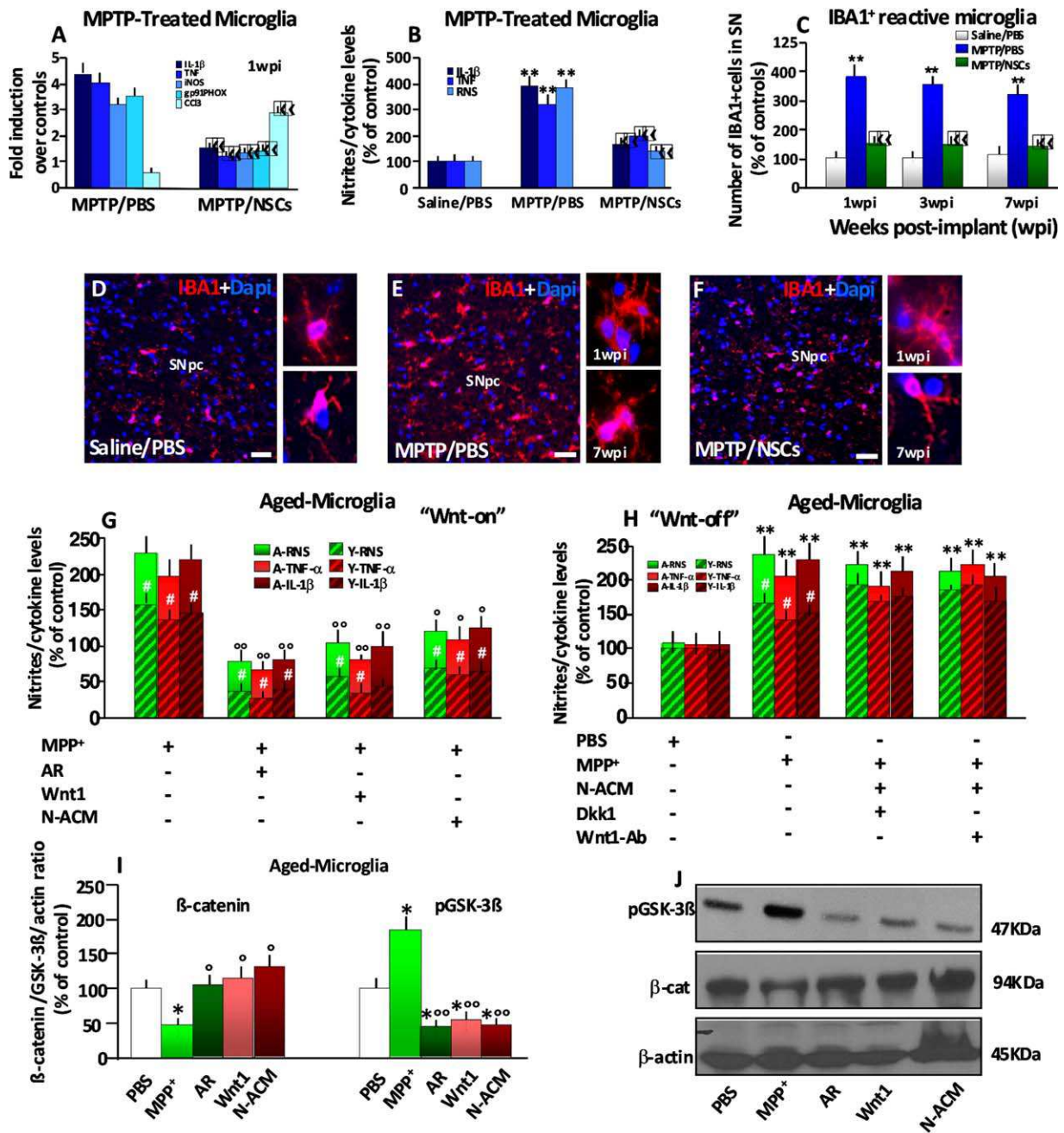


Figure 6. NSC grafts override the microglial pro-inflammatory status in vivo and reverse MPP⁺-induced microglial inflammatory mediators in vitro. **(A):** NSC grafts downregulate the expression levels of *IL-1 β* , *Nos2*, *g91Phox*, *TNF- α* , and *CCL3* by qRT-PCR, in microglia cell lysates versus MPTP/PBS-treated SN. **(B):** NSC grafts reversed the increased IL-1 β and TNF- α and RNS in microglial supernates. **(C):** NSC grafts reduce IBA1⁺/Dapi⁺ (stage 3–4) microglia cell numbers (percentage of controls) versus MPTP/PBS quantified at 1–7 wpi. **(D–F):** NSC grafts reverse MPTP-induced increased IBA1⁺/Dapi⁺ microglial cell numbers in midbrain sections at the level of the SNpc. Scale bars in (D): 100 μ m. **(G, H):** Aged microglia (A-micro) cultured in vitro and then challenged with MPP⁺ release higher levels of RNS, IL-1 β , and TNF- α , compared with younger (Y) glia (*dashed lines*) (G, H). Exposure to Wnt1, AR, or N-ACM (conditions "Wnt-on") before MPP⁺ treatment counteracts the release of pro-inflammatory mediators in both A- and Y-glia, although Y-glia (*dashed lines*) exert a stronger inhibition versus A-glia (G). Conversely, pretreatment of A/Y-micro with the Wnt-Anta, Dkk1 or Wnt1-Ab (conditions "Wnt-off"), applied before Wnt1 or N-ACM, efficiently reversed the downregulation of RNS, IL-1 β , TNF- α (H). **(I, J):** β -catenin and pGSK β expression as determined by wb analysis in A-glia. Differences (Mean \pm SEM values) were analyzed using ANOVA followed by the Newman–Keuls test. *, $p \leq .05$; **, $p \leq .01$ versus saline/PBS or PBS respectively; \circ , $p \leq .05$; $\circ\circ$, $p \leq .01$ versus MPTP or MPP⁺, within each treatment group respectively; #, $p \leq .05$ versus A-microglia, within each treatment group, respectively. Abbreviations: MPTP, 1-methyl-4-phenyl-1,2,3,6-tetrahydropyridine; NSC, neural stem/progenitor cells; PBS, phosphate buffered saline; wpi, weeks post-implant.

Accordingly, the pro-inflammatory mediators, IL-1 β , TNF- α , and RNS, were restored to levels comparable with those determined in MPTP/PBS mice (Fig. 7J–7M). Of note, qPCR

analysis of Wnt signaling genes performed by 1 wpi further indicated that Wnt-Ant reversed the NSC-induced increase in the Wnt canonical receptor, *Fzd1*, and Wnt-dependent

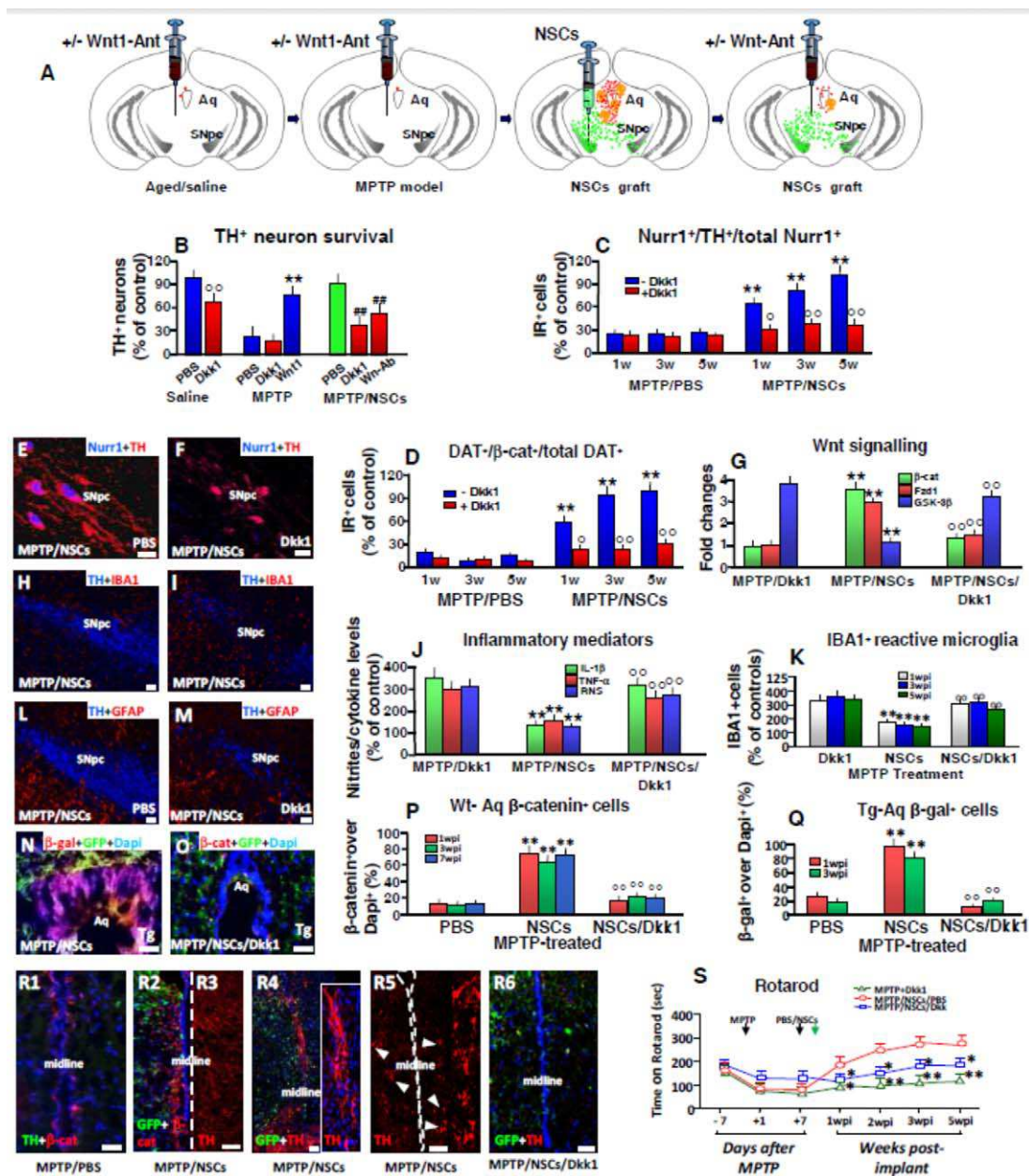


Figure 7. Wnt/ β -catenin signaling antagonism counteracts the therapeutic effects of NSC grafts on the SNpc and Aq-PVR of MPTP mice. **(A):** Scheme of the treatments. **(B):** Blockade of Wnt/ β -catenin signaling (Dkk1 or Wnt1-Ab) reverses NSC graft-induced increase of TH⁺ neuron survival at 5 wpi, whereas Wnt1 treatment promotes TH⁺ neuroprotection in MPTP mice. $^{\circ}$, $p < .01$ versus saline/PBS; ** , $p < .01$ versus MPTP/PBS and MPTP/Dkk1; $^{\#\#}$, $p < .01$ versus MPTP/NSC. **(C-E):** Dkk1 reverses NSC graft-induced increased Nurr1⁺/TH⁺ (C), DAT⁺/ β -cat⁺/total DAT⁺ (D) and Nurr1 expression (blue) (E-F) in SNpc (D). ** , $p < .01$ versus MPTP/PBS; $^{\circ}$, $p < .05$; $^{\circ\circ}$, $p < .01$ versus MPTP/NSCs without Dkk1 treatment. **(G):** Dkk1 reverses NSC graft-induced increased *Cttnb1* and *Fzd-1* mRNAs, while upregulating *GSK-3 β* , by qRT-PCR in SN. **(H-K):** Dkk1 increases stage 3–4 IBA1⁺ microglia in SNpc (H, I), quantified at 1–5 wpi (J) and reverses NSC graft-induced decreased levels of IL-1 β and TNF- α , and RNS (K). ** , $p < .01$ versus MPTP/Dkk1; $^{\circ}$, $p < .01$ versus MPTP/NSC. **(L, M):** Dkk1 reduces GFAP⁺ (red) astrocytes and TH⁺ (blue) neurons induced by the NSC graft (L). **(N-Q):** Dkk1 abolishes NSC grafts-induced transcriptionally active β -catenin in the Aq of β -catenin reporter mice (N, O). Dkk1 counteracts NSC graft-induced increased β -catenin⁺/DAPI⁺ (P) and β -gal⁺/DAPI⁺ (Q) cells in Aq. (N bar 100 μ m, O bar 50 μ m) ** , $p < .01$ versus PBS; $^{\circ}$, $p < .01$ versus MPTP/NSC. **(R1-R6):** Dkk1 abolishes NSC graft-induced increased β -catenin-IF and TH-IF along the Aq-PVRs. β -catenin (red) and TH (R1, bar: 100 μ m), β -catenin (red) and GFP (R2, bar: 200 μ m); TH (R3, R5, red, bar: 200 μ m) and TH + GFP (R4, R6, bar: 200 μ m). **(S):** Dkk1 reverses the increased motor performance of NSC mice. * , $p < .05$; ** , $p < .01$ versus MPTP/NSCs/PBS. Abbreviations: Aq, aqueduct; MPTP, 1-methyl-4-phenyl-1,2,3,6-tetrahydropyridine; NSC, neural stem/progenitor cells; PBS, phosphate buffered saline; SNpc, substantia nigra pars compacta; TH, tyrosine hydroxylase; wpi, weeks post-implant.

transcription factor, *Cttnb1*, to levels comparable with those determined in MPTP/PBS, whereas it upregulated the endogenous Wnt-ant *GSK-3 β* transcript levels (Fig. 7G).

We then sought to use transgenic (Tg) β -catenin (BATGAL) reporter mice [25, 79], which allow the visualization of cells with transcriptionally active Wnt/ β -catenin signaling through

the expression of nuclear β -galactosidase (β -gal) [25, 79]. When midbrain coronal sections at the level of the Aq-PVRs were stained with GFP, β -gal or β -catenin, coupled to Dapi nuclear staining, we found that NSC grafts promoted the accumulation of β -gal in GFP⁺ cells within the Aq-PVRs (Fig. 7N), with GFP⁺ cells appearing in close contact with β -gal⁺ cells, mirroring the distribution of GFP⁺GFAP⁺ shown in Figure 4I2–4I4. The quantitative analysis of the percentages of β -gal⁺/ β -catenin⁺/Dapi⁺ cells in Aq-PVRs also indicated that NSC grafts promoted an increase of (74.2% \pm 8.0%; 64.4% \pm 6.3%; and 73.0% \pm 7.5% at 1, 3 and 7 wpi respectively; $p \leq .01$) versus MPTP/PBS mice (Fig. 7N, 7P, 7Q).

On the contrary, in Wnt-Ant (Dkk1)-treated MPTP/NSC mice the number of β -catenin-expressing cells in Aq-PVR was significantly reduced (Fig. 7O–7Q), thus supporting Wnt signaling activation as a result of the NSC graft as opposed to failure of Wnt/ β -catenin signaling activation in Aq-PVRs of aged MPTP mice [25].

We also found that MPTP/NSC (Fig. 7R2–7R5) mice, but not in MPTP/PBS (Fig. 7R1) mice or MPTP/NSC mice treated with Dkk1 (Fig. 7R6), showed a sharp increase in β -catenin (R2) and TH immunoreactivity in neurons along the PVRs/midline (Fig. 7R3–7R5). Here, TH⁺ cell bodies with different morphologies and size were seen coursing along the midline down to the VTA of NSC grafted mice (R5), similar to what it is observed when TH⁺ neurons traffic from the Aq to the SNpc in younger MPTP mice during SNpc neurorepair [25]. In MPTP/NSC mice treated with Dkk1, we observed no TH⁺ neurons in Aq-PVRs (Fig. 7R6). These data demonstrate that NSC grafts activate β -catenin transcription, inducing a marked increase in TH⁺ cells within the Aq-PVR and VTA, and that this process is blocked by Wnt/ β -catenin antagonism.

By blocking the effects of NSCs on the brain of MPTP-treated mice, Dkk1 led to a significant ($p \leq .05$) inhibition of motor performance on the rotarod test, versus MPTP/NSC mice (Fig. 7R). Thus, Wnt/ β -catenin signaling activation by NSC grafts at the SNpc and Aq-PVR is required for NSC-promoted DA pathological and functional restoration of aged PD mice.

DISCUSSION

An increasing number of studies have confirmed the ability of transplanted NSCs to promote beneficial effects in rodent and primate models of PD, by targeting the injured microenvironment (and/or the endogenous NSC niches) acting mainly via trophic support and immunomodulatory effects, rather than directly differentiating into mDA neurons [62–68]. However, the mechanisms underlying the beneficial effects of NSCs have not been clarified yet. Because aging is the chief risk factor for PD development, we sought to focus on the aged male midbrain microenvironment to address the ability of NSCs to activate intrinsic cues that may instruct midbrain astrocytes to implement mDA neurorepair in MPTP-induced long-lasting DA neurotoxicity.

We report that SVZ-derived adult NSCs transplanted in the aged MPTP-injured SN promote a remarkable time-dependent endogenous nigrostriatal DA neurorestoration. Although multiple modes of reciprocal interactions between exogenous NSCs and the pathological host milieu may underlie the functional

improvement observed, our data suggest that NSCs and astrocyte-derived factors, especially Wnt1, might play a major role acting at different levels to rejuvenate the host microenvironment and promote mDA neurorestoration.

We found that NSC grafts elicited the expression of Wnt1 both in en- and ex-Astros, thereby favoring the protection of the imperilled/dysfunctional mDA neurons, via Wnt1/Fzd-1/ β -catenin signaling activation. Within the inflammatory microenvironment, NSC grafts, with the collaboration of astrocyte-derived factors, including Wnt1, switched the pro-inflammatory phenotype of microglial cells, providing further mDA neuroprotection. At the Aq-DA niche level, NSC grafts recapitulated a genetic Wnt1-dependent DA developmental program inciting the acquisition of mature Nurr1⁺ TH⁺ neuronal phenotype in post-mitotic DA precursors, thus increasing the endogenous pool of mDA neurons contributing to the reversal of MPTP-induced nigrostriatal toxicity.

NSC Grafts Restore Nigrostriatal DA Plasticity in the Aged MPTP Mouse Model of PD

With advancing age, the decline of the nigrostriatal DA system coupled with the progressive loss of mDA neuron adaptive potential are believed to contribute to the slow but inexorable nigrostriatal degeneration of PD [2, 7–10, 20, 21]. Although young adult rodents experience a time-dependent recovery/repair from MPTP insults, aging mice fail to recover for their entire lifespan [7–10]. With aging, gene–environment interactions further reduce the brain's self-adaptive potential, including DA compensatory mechanisms [2–19, 37–39, 43, 44, 89], with harmful consequences for neuron–glia crosstalk, mDA neuron plasticity and repair.

Here we found that, within the aged microenvironment, NSC grafts survived and proliferated within the SN of both sides in situ. A significant fraction of transplanted cells acquired an astrocytic phenotype both at the SN level and at the midbrain Aq-PVRs with a robust migration of NSCs to the Wnt-sensitive mDA progenitor niche, which is impaired in aging and MPTP exposure [25]. Interestingly, these effects were not observed when NSCs were transplanted into intact saline-injected controls, or when a mock cell graft was transplanted into MPTP mice, thus indicating the lesion—and NSC—graft specificity of the observed effects.

At the SN level, NSC grafts efficiently reversed aging and MPTP-induced downregulation of major DA transcripts, including *Th*, *Slc6a3* (DAT), *Slc18a2* (VMAT), and the DA-specific transcription factor *Nr4a2* (Nurr1), which is required for the survival of mDA neurons [80]. At the striatal level, NSC grafts promoted the recovery of DAT and TH immunoreactivity, increased synaptosomal DA uptake capacity and reversed motor impairment of aged MPTP mice. Together, these findings indicated the ability of NSC graft to restore the adaptive capacity of nigrostriatal DA neurons and to boost intrinsic cues within the midbrain microenvironment, thus reinstating DA functionality similar to what is observed in young male MPTP mice [25, 30].

The onset of PD symptoms is preceded by a slow mDA degeneration phase [2, 7–10, 20, 21]. Hence, the observed capability of NSC grafts to reactivate the MPTP-impaired DA neurons may suggest a therapeutic window of opportunity for mDA neurorestorative interventions aimed at protecting or enhancing the function of the remaining neurons, while augmenting latent intrinsic regenerative host mechanisms [68].

NSC Grafts Rejuvenate the Host Microenvironment via NSC–Glia–Neuron Crosstalk and Wnt/ β -Catenin Signaling

Within this scenario, reactive astrocytes emerge as key microenvironmental players in the injured brain exerting both beneficial and detrimental effects that have not yet been completely clarified [32–34, 36, 37]. Astrocytes are equipped with a robust anti-oxidant system and are known to protect neurons from oxidative stress and growth factor deprivation-induced cell death [32–35, 89]. Oxidative stress can indeed upregulate the expression of astrocytic NF-E2-related factor 2 (*Nrf2*), which translocates to the nucleus and binds to ARE [24]. Importantly, binding to ARE upregulates a cluster of anti-oxidant genes, including anti-oxidant, anti-inflammatory and cytoprotective genes, such as *Heme oxygenase1* (*Hmox1*) [24, 81], playing a prominent role for the vulnerable mDA neurons [32–34, 81, 89]. However, with aging, astrocytes become dysfunctional and the proinflammatory status is greatly exacerbated [11–19, 24, 89], likely resulting in the inhibition of the anti-oxidant [24], neuroprotective and proneurogenic capabilities of astrocytes.

We hypothesized that transplanted NSCs may have an impact on the aging of astrocytes, as well as on an integrated response of a variety of neighboring neural and non-neural (i.e., microglial) cell types [68]. Although from our qPCR analysis it is difficult to differentiate the exogenous NSC- versus the endogenous SN-expressed mRNAs, it seems plausible that the observed changes might result from a NSC to host SN crosstalk, resulting in the downregulation of the exacerbated levels of pro-inflammatory mediators, while increasing the transcription of anti-oxidant genes and certain chemokines demonstrated to directly activate Wnt signaling in both young and aged astrocytes [24, 25, 30]. Interestingly, NSC grafts promoted the expression of canonical Wnt1 signaling genes, including both direct and indirect Wnt/ β -catenin targets genes [38–41, 82–85].

Previous studies focusing on genetic networks recapitulating the early signals for the development of mDA neurons identified Wnt1 as a unique critical morphogen for mDA neurons, where activation of the Wnt1/ β -catenin signaling is required for mDA neuron specification [38–42, 97]. Of special interest, the sustained and ectopic expression of Wnt1 in genetically affected *En1* heterozygote (*En1*^{+/-}) mice can induce a neuroprotective Wnt1-dependent gene cascade promoting the survival of *En1* mutant (*En1*^{+/-} and *En1*^{-/-} mice) mDA neurons and rescuing them from premature cell death [39].

Our results are in line with previous findings underlying a chief pro-survival role of Wnt/ β -catenin signaling [28–30, 39, 43, 44, 49–53], and further suggest that this NSC graft-induced Wnt1 might drive a rescue effect in the aged SN microenvironment, acting on both the highly vulnerable mDA neurons, and on the exacerbated aged microglial inflammatory phenotype. We found that NSC-derived Wnt-expressing ex-Astro, but not Wnt-deficient (aged and/or TNF- α /IL-1 β -treated) endogenous Y-Astro and N-Astro, efficiently protected primary mesencephalic DA neurons from MPP⁺-induced Caspase-3-dependent TH⁺ neuron death, in vitro, whereas this neuroprotection was abolished by the Wnt-ant, thus indicating that Wnt/ β -catenin signaling activation is a critical determinant of ex-Astro- and en-Astro-induced TH neuroprotection. Conditioned media from NSC, despite having no effects of its own, it efficiently reversed the inability of aged

astrocytes to protect TH neurons, as did the Wnt-activating chemokine protocol. These findings suggest that factors released by NSCs, Wnt signaling and the inflammatory milieu influence glial–neuron interactions toward neuroprotection [43, 44, 89].

Reactive astrocytes were shown to turn into a highly cytotoxic phenotype when stimulated by LPS-activated microglia secreting proinflammatory cytokines, including IL-1 β and TNF- α , which inhibit the ability of astrocytes to promote neuronal survival, outgrowth, and synaptogenesis [36]. Additionally, a prolonged dysfunction of astrocytes and microglia activation have been shown to accelerate the degeneration of SNpc DA neurons, blocking the compensatory mechanisms of neuronal repair during early dysfunction induced by 6-OHDA lesion in rats [37]. Ageing represents a critical period whereby microglia are subject to structural deterioration/dystrophy, they vary their response to injury and increase the secretion of a plethora of proinflammatory mediators [11–19, 89]. These evidences support a critical role for aging-induced impairment of astrocyte–microglia crosstalk to MPTP-induced long-lasting mDA neurotoxicity.

Here, we further show that during aging, astrocyte dysfunction may result from a deregulated crosstalk with the “primed” MPTP-challenged microglia, which secretes excessive amounts of harmful pro-inflammatory mediators while reducing the expression of specific chemokines (e.g., CCL3 and CXCL11) and key astrocytic anti-oxidant factors (e.g., *Nrf2* and *Hmox1*). These mechanisms result in reduced Wnt1-dependent astrocyte neuroprotective, neurotrophic, and immunomodulatory activities.

Hence, in aged-microglia, a “Wnt-on” switch (e.g., Wnt1, GSK-3 β -antagonism, or N-ACM) efficiently reversed the up-regulated levels of TNF- α , IL1- β and RNS, whereas a “Wnt-off” condition (e.g., Wnt-ant) abolished the Wnt1-induced cytokine suppression. These in vitro findings therefore argued in favor of reciprocal NSC–astrocyte–microglial–neuron interactions, whereby Wnt/ β -catenin signaling appeared to fulfil the role of a common pathway toward neuroprotection.

NSC Grafts at the Aq-PVR DA Niche Promote the Activation of Wnt/ β -Catenin Signaling and the Differentiation of Nurr1⁺TH⁻ DA Precursors

An additional new finding of this study underlines the capability of NSC grafts to target the midbrain DA niche. We found that NSC grafts induced ex-Astro accumulation in high proportions at the Aq-PVRs, with upregulation of Wnt/ β -catenin target genes, mimicking the response of young MPTP mice [25].

Indeed, astrocyte-derived Wnts and β -catenin are recognized to control DA neurogenesis by maintaining the integrity of the neurogenic niche and promoting the progression from Nurr1⁺/TH⁻ post-mitotic progenitors to Nurr1⁺/TH⁺ neurons [25, 38–42, 97]. Here, we found that NSC grafts promoted progressive increases in Nurr1⁺/TH⁺ and DAT⁺/ β -catenin⁺ neurons, while this effect was counteracted by Wnt1-Ant treatment suggesting the involvement of a Wnt1-dependent mechanism [25]. In NSC-grafted, but not Wnt-Ant-treated mice, we observed numerous endogenous TH⁺ neurons with different sizes and morphologies, cursing along the Aq-PVRs and midline region “en route” to the VTA-SNpc. As a consequence, NSC graft treatment progressively increased the number of TH⁺ neurons accompanying nigrostriatal rescue and repair, whereas these processes were abolished by Wnt-Ant treatment.

Previous studies indicated that astrocyte-derived factors might play a role in enhancing the dopaminergic differentiation of stem cells and promoting brain repair in the MPTP-injured midbrain [25, 30, 88]. Currently, the neurogenic potential of DA neurons in the adult midbrain is a highly debated issue. Recent findings in 6-OHDA-lesioned rodents reported SN newborn DA neurons mainly derived from the migration and differentiation of the NSCs in the Aq-SVZ and their adjacent regions [98], but further studies are clearly needed to verify whether an NSC graft may activate neurogenesis in endogenous niches [62, 64, 65] and boost the production of newly born mDA neurons in the aged MPTP mouse brain.

CONCLUSION

We have shown that NSC grafts drive an astrocyte-dependent Wnt1 signaling activation resulting in a panel of neurotrophic and anti-inflammatory/anti-oxidant mechanism(s) that rejuvenate the aged inflammatory milieu and favor a neurorestorative program for mDA neurons. In light of the emerging picture implicating deregulated Wnt/ β -catenin signaling in PD [38–44, 50–57], our findings predict a novel perspective on harnessing Wnt/ β -catenin signaling with functionally plastic NSC grafts as a novel therapeutic strategy for PD.

STUDY APPROVAL

All studies were carried out in strict accordance with the Guide for the Care and Use of Laboratory Animals (NIH), approved by the Institutional Animal Care and Use Committee guidelines. All experimental procedures were approved by the OASI institutional Ethical Review Board. All surgeries were performed under anesthesia.

ACKNOWLEDGMENTS

We thank the Italian Ministry of Health (Ricerca Corrente, Grants 2013–2017, projects RCL13-RC014, RCL115, RCL16–17 to

B.M.) the Italian Ministry of Research and University (MIUR, to B.M.), The OASI (IRCCS) Institution Troina (EN) Italy, The BIOMETEC Department (University of Catania, Medical School, Catania, Italy), The Italian Multiple Sclerosis Association (AISM, Grant 2010//R/31 and Grant 2014/PMS/4 to S.P.), The United States Department of Defense (DoD) Congressionally Directed Medical Research Programs (DMRP) (Grant MS140019 to S.P.), The Italian Ministry of Health (GR-08-7 to S.P.), The European Research Council (ERC) under the SWRC-2010-StG grant agreement 260511-SEM-SEM, The Evelyn Trust (RG 69865 to S.P.), and a core Support Grant from the Wellcome Trust and MRC to the Wellcome Trust–Medical Research Council Cambridge Stem Cell Institute to S.P. L.P.J. and B.B. were supported by a Wellcome Trust Research Training Fellowship (RG79423).

AUTHOR CONTRIBUTIONS

F.L'E.: study design, performing experiments, collection of data, data analyses, manuscript writing, final approval of manuscript; C.T.: collection of data, data analyses, provision of study material, performing experiments, final approval of manuscript; L.P.-J.: data analysis and interpretation, manuscript writing, final approval of manuscript; M.F.S.: performing experiments, collection of data, data analysis and interpretation, manuscript writing, final approval of manuscript; N.T.: performing experiments, collection of data and data analyses, final approval of manuscript; S.C.: performed experiments, collection of data and data analyses, final approval of manuscript; B.B.: data analyses, provision of study material, final approval of manuscript; S.P. and B.M.: conception and design, data analysis and interpretation, manuscript writing, final approval of manuscript.

DISCLOSURE OF POTENTIAL CONFLICTS OF INTEREST

S.P. owns >5% of CITC Ltd. The other authors indicated no potential conflicts of interest.

REFERENCES

- Del Tredici K, Braak H. Lewy pathology and neurodegeneration in premotor Parkinson's disease. *Mov Disord* 2012;27:597–607.
- Hornykiewicz O. Parkinson's disease and the adaptive capacity of the nigrostriatal dopamine system: Possible neurochemical mechanisms. *Adv Neurol* 1993;60:140–147.
- Cannon JR, Greenamyre JT. Gene-environment interactions in Parkinson's disease: Specific evidence in humans and mammalian models. *Neurobiol Dis* 2013;57:38–46.
- Langston JW, Forno LS, Tetrad J. Evidence of active nerve cell degeneration in the substantia nigra of humans years after 1-methyl-4-phenyl-1,2,3,6-tetrahydropyridine exposure. *Ann Neurol* 1999;46:598–605.
- Lastres-Becker I, Ulusoy A, Innamorato NG. α Synuclein expression and Nrf2-deficiency cooperate to aggravate protein aggregation, neuronal death and inflammation in early-stage Parkinson's disease. *Hum Mol Genet* 2012;21:3173–3192.
- Liu HF, Ho PW, Leung GC et al. Combined LRRK2 mutation, aging and chronic low dose oral rotenone as a model of Parkinson's disease. *Sci Rep* 2017;7:40887.
- Rodriguez M, Rodriguez-Sabate C, Morales I et al. Parkinson's disease as a result of aging. *Aging Cell* 2015;14:293–308.
- De la Fuente-Fernández R, Schulzer M, Kuramoto L et al. Age-specific progression of nigrostriatal dysfunction in Parkinson's disease. *Ann Neurol* 2011;69:803–810.
- Collier TJ, Lipton J, Daley BF et al. Aging-related changes in the nigrostriatal dopamine system and the response to MPTP in nonhuman primates: Diminished compensatory mechanisms as a prelude to parkinsonism. *Neurobiol Dis* 2007;26:56–65.
- Branch SY, Sharma R, Beckstead MJ. Aging decreases L-Type calcium channel currents and pacemaker firing fidelity in substantia nigra dopamine neurons. *J Neurosci* 2014;34:9310–9318.
- Marchetti B, Abbracchio MP. To be or not to be (inflamed) is that the question in anti-inflammatory drug therapy of neurodegenerative diseases?. *Trends Pharmacol Sci* 2005;26:517–525.
- Hirsch EC, Hunot S. Neuroinflammation in Parkinson's disease: A target for neuroprotection?. *Lancet Neurol* 2009;8:382–397.
- Gao HM, Hong JS. Why neurodegenerative diseases are progressive: Uncontrolled inflammation drives disease progression. *Trends Immunol* 2008;29:357–365.
- Gao HM, Zhang F, Zhou H et al. Neuroinflammation and α -synuclein dysfunction potentiate each other, driving chronic progression of neurodegeneration in a mouse model of Parkinson's disease. *Environ Health Perspect* 2011;119:807–814.
- Przedborski S. Inflammation and Parkinson's disease pathogenesis. *Mov Disord* 2010;25:S55–S57.
- McGeer PL, McGeer EG. Glial reactions in Parkinson's disease. *Mov Disord* 2008;23:474–483.
- L'Episcopo F, Tirolo C, Testa N et al. Glia as a turning point in the therapeutic strategy

- of Parkinson's disease. *CNS Neurol Dis* 2010; 9:349–372.
- 18** L'Episcopo F, Tirolo C, Testa N et al. Switching the microglial harmful phenotype promotes lifelong restoration of substantia nigra dopaminergic neurons from inflammatory neurodegeneration in aged mice. *Rejuvenation Res* 2011;14:411–424.
- 19** Njjea EG, Boelen E, Stassen FR et al. Ex vivo cultures of microglia from young and aged rodent brain reveal age-related changes in microglial function. *Neurobiol Aging* 2012; 33:195.e1–12.
- 20** Bezard E, Gross CE. Compensatory mechanisms in experimental and human parkinsonism: Towards a dynamic approach. *Prog Neurobiol* 1998;55:93–116.
- 21** Zigmond MJ. Do compensatory processes underlie the preclinical phase of neurodegenerative diseases? Insight from an animal model of parkinsonism. *Neurobiol Dis* 1997;4:247–253.
- 22** Höglinger GU, Rizk P, Muriel MP et al. Dopamine depletion impairs precursor cell proliferation in Parkinson disease. *Nat Neurosci* 2004;7:726–735.
- 23** Luo J, Daniels SB, Lenington JB et al. The aging neurogenic subventricular zone. *Aging Cell* 2006;5:139–152.
- 24** L'Episcopo F, Tirolo C, Testa N et al. Aging-induced Nrf2-ARE pathway disruption in the subventricular zone (SVZ) drives neurogenic impairment in parkinsonian mice via PI3K-Wnt/ β -catenin dysregulation. *J Neurosci* 2013;33:1462–1485.
- 25** L'Episcopo F, Tirolo C, Testa N et al. Wnt/ β -catenin signaling is required to rescue midbrain dopaminergic progenitors and restore nigrostriatal plasticity in ageing mouse model of Parkinson's disease. *STEM CELLS* 2014;32:2147–2163.
- 26** Hermann A, Maisel M, Wegner F et al. Multipotent neural stem cells from the adult tegmentum with dopaminergic potential develop essential properties of functional neurons. *STEM CELLS* 2006;24:949–964.
- 27** Hermann A, Suess C, Fauser M et al. Rostro-caudal loss of cellular diversity within the periventricular regions of the ventricular system. *STEM CELLS* 2009;27:928–941.
- 28** Marchetti B, L'Episcopo F, Morale MC et al. Uncovering novel actors in astrocyte-neuron crosstalk in Parkinson's disease: The Wnt/ β -catenin signaling cascade as the common final pathway for neuroprotection and self-repair. *Eur J Neurosci* 2013;37:1550–1563.
- 29** L'Episcopo F, Serapide MF, Tirolo C et al. A Wnt1 regulated Frizzled-1/ β -catenin signaling pathway as a candidate regulatory circuit controlling mesencephalic dopaminergic neuron-astrocyte crosstalk: Therapeutical relevance for neuron survival and neuroprotection. *Mol Neurodegener* 2011;13:6–49.
- 30** L'Episcopo F, Tirolo C, Testa N et al. Reactive astrocytes and Wnt/ β -catenin signaling link nigrostriatal injury to repair in 1-methyl-4-phenyl-1,2,3,6-tetrahydropyridine model of Parkinson's disease. *Neurobiol Dis* 2011;41:508–527.
- 31** L'Episcopo F, Tirolo C, Testa N et al. Plasticity of subventricular zone neuroprogenitors in MPTP (1-methyl-4-phenyl-1,2,3,6-tetrahydropyridine) mouse model of Parkinson's disease involves crosstalk between inflammatory and Wnt/ β -catenin signaling pathways: Functional consequences for neuroprotection and repair. *J Neurosci* 2012;32:2062–2085.
- 32** Bélanger M, Magistretti PJ. The role of astroglia in neuroprotection. *Dialog Clin Neurosci* 2009;11:281–295.
- 33** Sofroniew MV, Vinters HV. Astrocytes: Biology and pathology. *Acta Neuropathol* 2010;119:7–35.
- 34** Booth HDE, Hirst WD, Wade-Martins R. The role of astrocyte dysfunction in Parkinson's disease pathogenesis. *Trend Neurosci* 2017;40:358–370.
- 35** L'Episcopo F, Drouin-Ouellet J, Tirolo C et al. GSK-3 β -induced Tau pathology drives hippocampal neuronal cell death in Huntington's disease: Involvement of astrocyte-neuron interactions. *Cell Death Dis* 2016;7:e2206.
- 36** Liddel SA, Guttenplan KA, Clarke LE et al. Neurotoxic reactive astrocytes are induced by activated microglia. *Nature* 2017; 541:481–487.
- 37** Kuter K, Olech L, Glowacka U. Prolonged dysfunction of astrocytes and activation of microglia accelerate degeneration of dopaminergic neurons in the rat substantia nigra and block compensation of early motor dysfunction induced by 6-OHDA. *Mol Neurobiol* 2018;55:3049–3066.
- 38** Wurst W, Prakash N. Wnt-1 regulated genetic networks in midbrain dopaminergic neuron development. *J Mol Cell Biol* 2014;6: 34–41.
- 39** Zhang J, Gotz S, Vogt Weisenhorn DM et al. A WNT1-regulated developmental gene cascade prevents dopaminergic neurodegeneration in adult En1(+/-) mice. *Neurobiol Dis* 2015;82:32–45.
- 40** Arenas E. Wnt signaling in midbrain dopaminergic neuron development and regenerative medicine for Parkinson's disease. *J Mol Cell Bio* 2014;6:42–53.
- 41** Joksimovic M, Awatramani R. Wnt/ β -catenin signaling in midbrain dopaminergic neuron specification and neurogenesis. *J Mol Cell Biol* 2014;6:27–33.
- 42** Parish CL, Thompson LH. Modulating Wnt signaling to improve cell replacement therapy for Parkinson's disease. *J Mol Cell Biol* 2014;6:54–63.
- 43** Marchetti B, Pluchino S. Wnt your brain be inflamed? Yes, it Wnt!. *Trends Mol Med* 2013;19:144–156.
- 44** L'Episcopo F, Tirolo C, Caniglia S et al. Targeting Wnt signaling at the neuroimmune interface in dopaminergic neuroprotection/repair in Parkinson's disease. *J Mol Cell Biol* 2014;6:13–26.
- 45** Okamoto M, Inoue K, Iwamura H et al. Reduction in paracrine Wnt3 factors during aging causes impaired adult neurogenesis. *FASEB J* 2011;25:3570–3582.
- 46** Miranda CJ, Braun L, Jiang Y et al. Aging brain microenvironment decreases hippocampal neurogenesis through Wnt-mediated survivin signalling. *Aging Cell* 2012;11:542–552.
- 47** Seib DRM, Corsini NS, Ellwanger K et al. Loss of Dickkopf-1 restores neurogenesis in old age and counteracts cognitive decline. *Cell Stem Cell* 2013;12:204–214.
- 48** Elzi DJ, Song M, Hakala K et al. Wnt antagonist SFRP1 functions as a secreted mediator of senescence. *Mol Cell Biol* 2012; 32:4388–4399.
- 49** Maiese K, Li F, Chong ZZ et al. The Wnt signalling pathway: Aging gracefully as a protectionist? *Pharmacol Ther* 2008;118:58–81.
- 50** Berwick DC, Harvey K. The importance of Wnt signalling for neurodegeneration in Parkinson's disease. *Biochem Soc Trans* 2012; 40:1123–1128.
- 51** Galli S, Lopes DM, Ammari R et al. Deficient Wnt signalling triggers striatal synaptic degeneration and impaired motor behaviour in adult mice. *Nat Commun* 2014;5:4992.
- 52** Harvey K, Marchetti B. Regulating Wnt signaling: A strategy to prevent neurodegeneration and induce regeneration. *J Mol Cell Biol* 2014;6:1–2.
- 53** Inestrosa NC, Arenas E. Emerging role of Wnts in the adult nervous system. *Nat Rev Neurosci* 2010;11:77–86.
- 54** Berwick DC, Javaheri B, Wetzel A et al. Pathogenic LRRK2 variants are gain-of-function mutations that enhance LRRK2-mediated repression of β -catenin signaling. *Mol Neurodegener* 2017;12:9.
- 55** Salašová A, Yokota C, Potěšil D et al. A proteomic analysis of LRRK2 binding partners reveals interactions with multiple signaling components of the WNT/PCP pathway. *Mol Neurodegener* 2017;12:54.
- 56** Berwick DC, Harvey K. The regulation and deregulation of Wnt signalling by PARK genes in health and disease. *J Mol Cell Biol* 2014;6:3–12.
- 57** Lee H, James WS, Cowley SA. LRRK2 in peripheral and central nervous system innate immunity: Its link to Parkinson's disease. *Biochem Soc Trans* 2017;45:131–139.
- 58** Olanow CW, Schapira AHV, Agid Y. Neurodegeneration and prospects for neuroprotection and rescue in Parkinson's disease. *Ann Neurol* 2003;53:S1.
- 59** Bacigaluppi M, Russo GL, Peruzzotti-Jametti L et al. Neural stem cell transplantation induces stroke recovery by upregulating glutamate transporter GLT-1 in astrocytes. *J Neurosci* 2016;36:10529–10544.
- 60** Cusimano M, Bizziato D, Brambilla E et al. Transplanted neural stem/precursor cells instruct phagocytes and reduce secondary tissue damage in the injured spinal cord. *Brain* 2012;135:447–460.
- 61** Pluchino S, Zanotti L, Rossi B et al. Neurosphere-derived multipotent precursors promote neuroprotection by an immunomodulatory mechanism. *Nature* 2005;436:266–471.
- 62** Zuo F, Xiong F, Wang X et al. Intrastriatal transplantation of human neural stem cells restores the impaired subventricular zone in Parkinsonian mice. *STEM CELLS* 2017;35:1519–1531.
- 63** Zuo F, Bao XJ, Sun XC et al. Transplantation of human neural stem cells in a Parkinsonian model exerts neuroprotection via regulation of the host microenvironment. *Int J Mol Sci* 2015;16:26473–26492.
- 64** Madhavan L, Daley BF, Sortwell CE et al. Endogenous neural precursors influence grafted neural stem cells and contribute to neuroprotection in the parkinsonian rat. *Eur J Neurosci* 2012;35:883–895.
- 65** Madhavan L, Daley BF, Paumier KL et al. Transplantation of subventricular zone neural precursors induces an endogenous precursor

cell response in a rat model of Parkinson's disease. *J Comp Neurol* 2009;515:102–115.

66 Redmond DE Jr., Bjugstad KB, Teng YD et al. Behavioral improvement in a primate Parkinson's model is associated with multiple homeostatic effects of human neural stem cells. *Proc Natl Acad Sci USA* 2007;104:12175–12180.

67 Yasuhara T, Matsukawa N, Hara K et al. Transplantation of human neural stem cells exerts neuroprotection in a rat model of Parkinson's disease. *J. Neurosci* 2006;26:12497–12511.

68 Ourednik J, Ourednik V, Lynch WP et al. Neural stem cells display an inherent mechanism for rescuing dysfunctional neurons. *Nat Biotechnol* 2002;20:1103–1110.

69 Jackson-Lewis V, Przedborski S. Protocol for the MPTP model of Parkinson's disease. *Nat Prot* 2007;2:141–151.

70 Franklin KBJ, Paxinos G. *The Mouse Brain in Stereotaxic Coordinates*. San Diego, CA: Academic Press Inc, 1997).

71 Baquet ZC, Williams D, Brody J et al. A comparison of model-based (2D) and design-based (3D) stereological methods for estimating cell number in the substantia nigra pars compacta of the C57BL/6J mouse. *Neuroscience* 2009;161:1082–1090.

72 Abercrombie M. Estimation of nuclear population from microtome sections. *Anat Rec* 1946;94:239–247.

73 Burke RE, Cadet JL, Kent JD et al. An assessment of the validity of densitometric measures of striatal tyrosine hydroxylase-positive fibers: Relationship to apomorphine-induced rotation in 6-hydroxydopamine lesioned rats. *J Neurosci Meth* 1990;35:63–73.

74 Morale MC, Serra PA, Delogu MR et al. Glucocorticoid receptor deficiency increases vulnerability of the nigrostriatal dopaminergic system: Critical role of glial nitric oxide. *FASEB J* 2004;18:164–166.

75 Gennuso F, Ferneti C, Tirolo C et al. Bilirubin protects astrocytes from its own toxicity inducing up-regulation and translocation of multidrug resistance-associated protein 1 (Mrp 1). *Proc Natl Acad Sci USA* 2004;101:2470–2475.

76 Gallo F, Morale MC, Spina-Purrello V et al. Basic fibroblast growth factor (bFGF) acts on both neurons and glia to mediate the neurotrophic effects of astrocytes on

LHRH neurons in culture. *Synapse* 2000;36:233–253.

77 Schwartz JP, Wilson DJ. Preparation and characterization of type 2 astrocytes cultured from adult rat cortex, cerebellum, and striatum. *Glia* 1992;5:75–80.

78 L'Episcopo F, Tirolo C, Caniglia S. Combining nitric oxide release with anti-inflammatory activity preserves nigrostriatal dopaminergic innervation and prevents motor impairment in a 1-methyl-4-phenyl-1,2,3,6-tetrahydropyridine model of Parkinson's disease. *J Neuroinflammation* 2010;7:83.

79 Maretto S, Cordenonsi M, Dupont S et al. Mapping Wnt/beta-catenin signaling during mouse development and in colorectal tumors. *Proc Natl Acad Sci USA* 2003;100:3299–3304.

80 Kadhodaei B, Ito T, Joodmardi E et al. Nurr1 is required for maintenance of maturing and adult midbrain dopamine neurons. *J Neurosci* 2009;29:15923–15932.

81 Chen PC, Vargas MR, Pani AK et al. Nrf2-mediated neuroprotection in the MPTP mouse model of Parkinson's disease: Critical role for the astrocyte. *Proc Natl Acad Sci USA* 2009;106:2933–2938.

82 Hoekstra EJ, von Oerthel L, van der Heider LP et al. Lmx1a encodes a rostral set of mesodiencephalic dopaminergic neurons marked by the Wnt/B-catenin signaling activator R-spondin 2. *PLoS One* 2013;8:e74049.

83 Chamorro MN, Schwartz DR, Vonica A et al. FGF-20 and DKK1 are transcriptional targets of beta-catenin and FGF-20 is implicated in cancer and development. *EMBO J* 2005;24:73–84.

84 Chung S, Leung A, Han BS et al. Wnt1-Lmx1a forms a novel auto-regulatory loop and controls midbrain dopaminergic differentiation synergistically with the SHH-FoxA2 pathway. *Cell Stem Cell* 2009;5:646–658.

85 Castelo-Branco G, Sousa KM, Bryia V et al. Ventral midbrain glia express region-specific transcription factors and regulate dopaminergic neurogenesis through Wnt-5a secretion. *Mol Cell Neurosci* 2006;31:251–262.

86 Sandhu JK, Gardaneh M, Iwasiew R et al. Astrocyte-secreted GDNF and glutathione antioxidant system protect neurons against 6-OHDA cytotoxicity. *Neurobiol Dis* 2009;33:405–414.

87 Cahoy JD, Emery B, Kaushal A et al. A transcriptome database for astrocytes,

neurons, and oligodendrocytes: A new resource for understanding brain development and function. *J Neurosci* 2008;28:264–278.

88 Yang F, Liu Y, Tu J et al. Activated astrocytes enhance the dopaminergic differentiation of stem cells and promote brain repair through bFGF. *Nat Commun* 2014;5:5627.

89 L'Episcopo F, Tirolo C, Serapide MF et al. Microglia polarization, gene-environment interactions and Wnt/ β -catenin Signalling: Emerging roles of glia-neuron and glia-stem/neuroprogenitor crosstalk for dopaminergic neurorestoration in aged parkinsonian brain. *Front Aging Neurosci* 2018;10:12.

90 Kreutzberg GW. Microglia: A sensor for pathological events in the CNS. *Trends Neurosci* 1996;19:312–318.

91 Streit WJ, Mrak RE, Griffin WS. Microglia and neuroinflammation: A pathological perspective. *J Neuroinflammation* 2004;1:14.

92 Schaale K, Neumann J, Schneider D et al. Wnt signaling in macrophages: Augmenting and inhibiting mycobacteria-induced inflammatory responses. *Eur J Cell Biol* 2011;90:553–559.

93 Ma B, Hottiger MO. Crosstalk between Wnt/ β -catenin and NF- κ B signaling pathway during inflammation. *Front Immunol* 2016;7:378.

94 Halleskog C, Schulte G. WNT-3A and WNT-5A counteract lipopolysaccharide-induced pro-inflammatory changes in mouse primary microglia. *J Neurochem* 2013;125:803–808.

95 Shang YC, Chong ZZ, Wang S et al. Prevention of β -amyloid degeneration of microglia by erythropoietin depends on Wnt1, the PI 3-K/mTOR pathway, Bad, and Bcl-xL. *Aging* 2012;4:187–201.

96 Chong ZZ, Li F, Maiese K. Cellular demise and inflammatory microglial activation during beta-amyloid toxicity are governed by Wnt1 and canonical signalling pathways. *Cell Signal* 2007;19:1150–1162.

97 Toledo EM, Gyllborg D, Arenas E. Translation of WNT developmental programs into stem cell replacement strategies for the treatment of Parkinson's disease. *Br J Pharmacol* 2017;174:4716–4724.

98 Xie MQ, Chen ZC, Zhang P et al. Newborn dopaminergic neurons are associated with the migration and differentiation of SVZ-derived neural progenitors in a 6-OHDA-injected mouse model. *Neuroscience* 2017;352:64–78.



See www.StemCells.com for supporting information available online.